Pharmacological Research 103 (2016) 26–48

Contents lists available at ScienceDirect

Pharmacological Research

journal homepage: www.elsevier.com/locate/yphrs

Invited review

Classification of small molecule protein kinase inhibitors based upon the structures of their drug-enzyme complexes

Robert Roskoski Jr.*

Blue Ridge Institute for Medical Research, 3754 Brevard Road, Suite 116, Box 19, Horse Shoe, NC 28742-8814, United States

ARTICLE INFO

Article history:
Received 25 October 2015
Received in revised form 26 October 2015
Accepted 27 October 2015
Available online 31 October 2015

Chemical compounds studied in this article:
Afatinib (PubMed CID: 10184653)
Crizotinib (PubMed CID: 11626560)
Erlotinib (PubMed CID: 176870)
Gefitinib (PubMed CID: 123631)
Imatinib (PubMed CID: 5291)
Nilotinib (PubMed CID: 644241)
Sorafinib (PubMed CID: 216239)
Sunitinib (PubMed CID: 5329102)
Tofacitinib (PubMed CID: 9926791)
Vemurafenib (PubMed CID: 42611257)

Keywords:
ATP-binding site
Catalytic spine
K/E/D/D
Protein kinase structure
Regulatory spine
Residence time

ABSTRACT

Because dysregulation and mutations of protein kinases play causal roles in human disease, this family of enzymes has become one of the most important drug targets over the past two decades. The X-ray crystal structures of 21 of the 27 FDA-approved small molecule inhibitors bound to their target protein kinases are depicted in this paper. The structure of the enzyme-bound antagonist complex is used in the classification of these inhibitors. Type I inhibitors bind to the active protein kinase conformation (DFG-Asp in, αC-helix in). Type I½ inhibitors bind to a DFG-Asp in inactive conformation while Type II inhibitors bind to a DFG-Asp out inactive conformation. Type I, I½, and type II inhibitors occupy part of the adenine binding pocket and form hydrogen bonds with the hinge region connecting the small and large lobes of the enzyme. Type III inhibitors bind next to the ATP-binding pocket and type IV inhibitors do not bind to the ATP or peptide substrate binding sites. Type III and IV inhibitors are allosteric in nature. Type V inhibitors bind to two different regions of the protein kinase domain and are therefore bivalent inhibitors. The type I–V inhibitors are reversible. In contrast, type VI inhibitors bind covalently to their target enzyme. Type I, I½, and II inhibitors are divided into A and B subtypes. The type A inhibitors bind in the front cleft, the back cleft, and near the gatekeeper residue, all of which occur within the region separating the small and large lobes of the protein kinase. The type B inhibitors bind in the front cleft and gate area but do not extend into the back cleft. An analysis of the limited available data indicates that type A inhibitors have a long residence time (minutes to hours) while the type B inhibitors have a short residence time (seconds to minutes). The catalytic spine includes residues from the small and large lobes and interacts with the adenine ring of ATP. Nearly all of the approved protein kinase inhibitors occupy the adenine-binding pocket; thus it is not surprising that these inhibitors interact with nearby catalytic spine (CS) residues. Moreover, a significant number of approved drugs also interact with regulatory spine (RS) residues.

Contents

Abbreviations: ALL, acute lymphoblastic leukemia; AS, activation segment; CDK, cyclin-dependent kinase; CML, chronic myelogenous leukemia; CS or C-spine, catalytic spine; EGFR or ErbB1, epidermal growth factor receptor; FGFR, fibroblast growth factor receptor; GIST, gastrointestinal stromal tumor; HER 2, human epidermal growth factor receptor-2 or human ErbB2; HGFR or c-Met, hepatocyte growth factor receptor; HP, hydrophobic; JAK, Janus kinase; NSCLC, non-small cell lung cancer; PDGFR, platelet-derived growth factor receptor; Ph^+, Philadelphia chromosome positive; PKA, protein kinase A; pY, phosphotyrosine; RCC, renal cell carcinoma; RS or R-spine, regulatory spine; Sh, shell.

* Fax: +1 828 890 8130.
E-mail address: rrj@brimr.org

http://dx.doi.org/10.1016/j.phrs.2015.10.021
1043-6618/

1. The protein kinase enzyme family

Protein kinases are enzymes that play key regulatory roles in nearly every aspect of cell biology [1]. These enzymes participate in signal transduction modules that regulate apoptosis, cell cycle progression, cytoskeletal rearrangement, differentiation, development, the immune response, nervous system function, and transcription. Protein kinases represent attractive drug targets because their dysregulation occurs in a variety of illnesses including cancer, diabetes, and autoimmune, cardiovascular, inflammatory, and nervous disorders. Both academic and commercial enterprises have expended considerable effort to determine the physiological and pathological functions of protein-kinase signal transduction pathways during the past 45 years.

Protein kinases catalyze the following reaction:

$$MgATP^{1-} + protein{-}O:H \rightarrow protein{-}O:PO_3{}^{2-} + MgADP + H^+$$

Based upon the nature of the phosphorylated —OH group, these enzymes are classified as protein-serine/threonine kinases and protein-tyrosine kinases. Manning et al. identified 478 typical and 40 atypical human protein kinase genes (total 518) that correspond to nearly 2% of all human genes [1]. Moreover, there are 106 protein kinase pseudogenes. The protein kinase family includes 385 serine/threonine kinases, 90 protein-tyrosine kinases, and 43 tyrosine-kinase like proteins. Of the 90 protein-tyrosine kinases, 58 are receptors with an extracellular, transmembrane, and intracellular domain and 32 are non-receptors occurring intracellularly. There is a small group of enzymes, which includes MEK1 and MEK2, that catalyze the phosphorylation of both threonine and tyrosine on target proteins. These intracellular proteins, which closely resemble and are classified as serine/threonine kinases, are called dual specificity kinases. Families of protein phosphatases catalyze the dephosphorylation of proteins [2,3] thus making phosphorylation–dephosphorylation an overall reversible process.

Because dysregulation and mutations of protein kinases play causal roles in human illnesses, this family of enzymes has become one of the most important drug targets over the past two decades [4], perhaps accounting for a quarter of all current drug discovery research and development efforts. Imatinib was the first small molecule targeted protein kinase inhibitor that was FDA-approved for the treatment of chronic myelogenous leukemia (CML) in 2001. The current list of FDA-approved drugs includes 27 orally effective direct protein kinase inhibitors that target a limited number of enzymes (Table 1). Most of these drugs are used for the treatment of malignancies except for ruxolitinib, which is used for the treatment of myelofibrosis, and tofacitinib, which is used for the treatment of rheumatoid arthritis. See www.brimr.org/PKI/PKIs.htm for the structures and selected properties of all currently FDA-approved protein kinase antagonists.

Nearly all of the approved protein kinase antagonists are steady-state competitive enzyme inhibitors with respect to ATP and they interact with the ATP-binding pocket. Targeting the ATP-binding site of protein kinases was not thought to be selective or effective because of the large number of protein kinases and other ATP-requiring enzymes with the likelihood that these binding sites would be indistinguishable thereby leading to numerous side effects [5]. However, the approval of imatinib for the effective treatment of chronic myelogenous leukemia dispelled this notion. As discussed later, structural studies have exploited differences within the ATP-binding site and contiguous regions that can be used to provide specificity for protein kinase inhibitors. As with the case of G-protein coupled receptors, the lesson to be relearned from these observations is that drugs can be tailored to bind specifically to targets that exhibit only subtle differences.

2. Structures of active and inactive protein kinases

2.1. The bilobed protein kinase domain and the K/E/D/D signature motif

We consider first the conformation of the active EGFR protein kinase domain as a prototype for all protein kinases. These domains have a small N-terminal lobe and a large C-terminal lobe that contain several conserved α-helices and β-strands (Fig. 1), first described by Knighton and co-workers for PKA [6,7]. The small lobe is dominated by a five-stranded antiparallel β-sheet (β1–β 5) and an αC-helix that contains a glutamate that makes a salt bridge with a lysine in the β3-sheet in the active conformation [8]. The small lobe contains a conserved glycine-rich (GxGxxG) ATP-phosphate-binding loop that occurs between the β1- and β2-strands. The G-rich loop helps position the β- and γ-phosphates of ATP for catalysis. The β1- and β2-strands harbor the adenine component of ATP.

The glycine-rich loop is followed by a conserved valine within the β2-strand that makes a hydrophobic contact with the adenine of ATP. The β3-strand typically contains an Ala-Xxx-Lys sequence, the lysine of which couples the α- and β-phosphates of ATP to the αC-helix. A conserved glutamate occurs near the center of the αC-helix within the small lobe of protein kinases. The presence of a salt-bridge between the β3-lysine and the αC-glutamate is a prerequisite for the formation of the active state and usually, but not always, corresponds to the "αC-in" conformation; by contrast the β3-lysine and the αC-glutamate of the dormant form of EGFR fail to make contact in the "αC-out" conformation (Fig. 1C). The αC-in

Table 1
Selected drug targets of FDA-approved protein kinase inhibitors.[a]

Drug target	Protein substrate	Receptor	Drug
ALK	Tyrosine	Yes	Crizotinib, ceritinib
BCR–Abl	Tyrosine	No	Bosutinib, dasatinib, imatinib, nilotinib, ponatinib
EGFR family	Tyrosine	Yes	Gefitinib, erlotinib, lapatinib, vandetanib, afatinib
PDGFRα/β	Tyrosine	Yes	Axitinib, gefitinib, imatinib, lenvatinib, nintedanib, pazopanib, regorafenib, sorafenib, sunitinib
VEGFRfamily	Tyrosine	Yes	Axitinib, lenvatinib, nintedanib, regorafenib, pazopanib, sorafenib, sunitinib
c-Met	Tyrosine	Yes	Crizotinib, cabozantinib
RET	Tyrosine	Yes	Vandetanib
BTK	Tyrosine	No	Ibrutinib
JAK family	Tyrosine	No	Ruxolitinib, tofacitinib
Src family	Tyrosine	No	Bosutinib, dasatinib, ponatinib, vandetanib
CDK family	Serine/threonine	No	Palbociclib, sorafenib
B-Raf	Serine/threonine	No	Vemurafenib, dabrafenib
MEK1/2	Dual specificity	No	Trametinib

[a] Adapted from www.brimr.org/PKI/PKIs.htm.

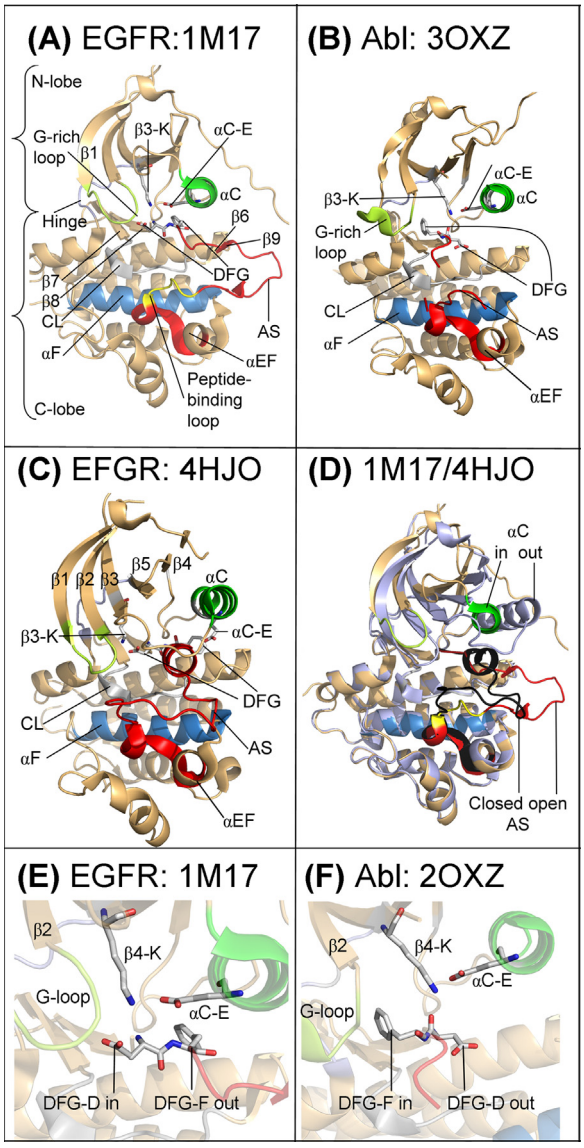

Fig. 1. (A) Active conformation of EGFR with DFG-D pointing inward toward the active site and the αC-helix directed inward toward both the β3-K and N-terminal region of the activation segment. (B) Inactive DFG-D out conformation. (C) Inactive DFG-D in and αC-helix out conformation. (D) Superposition of active αC-helix in (1M17) and inactive αC-helix out (4HJO) conformations. (E) Active EGFR with DFG-D directed inward toward the active site. (F) Inactive Abl with DFG-D directed outward from the active site. The human enzyme and corresponding PDB ID are listed. AS, activation segment; CL, catalytic loop. Figs. 1, 2, 5, and 7 were prepared using the PyMOL Molecular Graphics System Version 1.5.0.4 Schrödinger, LLC.

conformation is necessary, but not sufficient, for the expression of full kinase activity.

The large lobe of protein kinase domains including that of EGFR is mainly α-helical with six conserved segments (αD-αI) [8]. The large lobe also contains four short conserved β-strands (β6–β9) that contain most of the catalytic residues associated with the phosphoryl transfer from ATP to its substrates. The αE-helix is followed by the β6-stand, the catalytic loop, the β7- and β8-strands, and the activation segment, which contains the β9-strand. The activation segment in the active state forms an open structure extending away from the catalytic loop that allows protein/peptide substrate binding. The dormant and the active protein kinase domains contain an additional αEF-helix near the end of the activation segment (Fig. 1A).

Hanks et al. aligned the catalytic domains of 65 protein kinases and identified 11 subdomains (I–XI) within the catalytic core of these enzymes with conserved amino-acid-residue signatures [9]. We selected a K/E/D/D (Lys/Glu/Asp/Asp) signature to exemplify the catalytic properties of protein kinases. As noted above, an invariant β3-strand lysine (the K of K/E/D/D) forms salt bridges with the αC-glutamate (the E of K/E/D/D). The catalytic loops surrounding the actual site of phosphoryl transfer differ in protein-serine/threonine and protein-tyrosine kinases. This loop is made up of a YRDLKPEN in the protein kinase AGC family, HRDLKPQN for other protein-serine/threonine kinases, HRDLAARN in receptor protein-tyrosine kinases, and HRDLRAAN for non-receptor protein-tyrosine kinases [9].

The catalytic loop aspartate, which is the first D of K/E/D/D), serves as a base that abstracts a proton from the protein —OH group of the substrate thereby facilitating the nucleophilic attack of the hydroxyl group onto the γ-phosphorous atom of ATP. The second aspartate of K/E/D/D constitutes the first residue of the so-called activation segment. In the majority of protein kinases, this segment begins with DFG (Asp-Phe-Gly) and ends with APE (Ala-Pro-Glu). Although the activation segment of EGFR begins with DFG, it ends with ALE (Ala-Leu-Glu). The difference between active and dormant conformations has received considerable emphasis in the characterization of protein kinases and the DFG-Asp in configuration represents the active conformation. However, dormant EGFR also occurs with the DFG-Asp in configuration. The DFG-Asp binds Mg^{2+}, which in turn coordinates the α- β- and γ-phosphates of ATP. The primary structure of the catalytic HRD loop occurs before the β7- and β8-strands, which are followed by the activation segment. The large lobe characteristically binds the peptide/protein substrates at a binding loop within the activation segment (Fig. 1A).

The configuration of the activation segment controls both substrate binding and catalysis [10]. Moreover, the initial five residues of the activation segment make up the magnesium-positioning loop. The activation segment in EGFR contains a phosphorylatable

tyrosine. The magnesium-positioning loop, the amino-terminus of the αC-helix, and the conserved HRD component of the catalytic loop are close together in the tertiary structure. In the analysis of the structures of some two dozen active protein kinases, Nolan et al. reported that phosphorylation of one or more residues within the activation segment is required for activation [11]. However, such phosphorylation is not required for the activation of EGFR [12,13].

Although the tertiary structure of catalytically active protein kinase domains are similar, Huse and Kuriyan noted that the crystal structures of dormant enzymes reveal distinct inactive conformations [14]. One of the most common inactive enzyme forms is the DFG-Asp out conformation. When this aspartate is directed outward, the DFG-F is directed into the active site (Fig. 1B). Fig 1E depicts the active DFG-D in configuration and Fig. 1F shows the inactive DFG-D out conformation. Another commonly occurring inactive conformation is the αC-helix out state (Fig. 1C) [10]. The superposition of an active enzyme and the αC-helix out conformation illustrates the differences in these two states (Fig. 1D). Also note that the activation segment in the αC-out conformation is in an inactive closed state. To summarize, the three main regulatory elements within the kinase domain include the N-terminal lobe αC-helix (αC-in, active; αC-out, inactive), the C-terminal lobe DFG-Asp (DFG-Asp in, active; DFG-Asp out, inactive), and the C-terminal lobe activation segment (AS open, active; AS closed, inactive). We also consider the structure of the regulatory spine, which is considered in the next section. It has a near linear structure in the active state and a distorted conformation in the inactive state.

2.2. Structures of the hydrophobic spines in active and dormant protein kinase domains

Kornev and co-workers compared the structures of the active and inactive conformations of 23 protein kinases and determined functionally important residues by a local spatial pattern alignment algorithm [15,16]. Their analysis led to the description of the structural skeletons of eight hydrophobic residues that constitute a catalytic or C-spine and four hydrophobic residues that constitute a regulatory or R-spine. Each spine consists of amino acids occurring in both the small amino-terminal lobe and the large carboxyterminal lobe. The regulatory spine contains residues from the αC-helix and the activation segment, both of which are important in characterizing active and dormant states. The adenine base of ATP is one component of the catalytic spine. The regulatory spine positions the protein substrate and the catalytic spine positions ATP thereby enabling catalysis. The structure of the spines differs between the active and dormant enzyme states and their correct alignment is necessary for the assembly of an active protein kinase domain.

The protein kinase regulatory spine consists of a residue from the beginning of the β4-strand, from the C-terminal end of the αC-helix, the phenylalanine of the activation segment DFG, along with the H/YRD-His/Tyr of the catalytic loop. The spinal component from the αC-helix is four residues C-terminal to the conserved αC-glutamate. The backbone of the catalytic loop histidine/tyrosine is anchored to the αF-helix by a hydrogen bond to a conserved aspartate residue within the αF-helix. Going from the aspartate within the αF-helix up to the top residue within the β4-strand, Meharena et al. labeled the residues RS0, RS1, RS2, RS3, and RS4 (Figs. 2 and 3) [10].

The regulatory spine of active protein kinase domains is nearly linear (Fig. 2A) while that of the dormant enzymes possesses various distortions. In the inactive DFG-Asp out form, the DFG-F residue (RS2) is displaced into the active site and separated from RS3/4; this form of the spine is broken (Fig. 2B). In the αC-helix out conformation, RS3 is displaced away from the active site along with the αC-helix (Fig. 2C). Besides these inactive forms, Meharena et al. described two less common inactive forms [10]. In the inactive

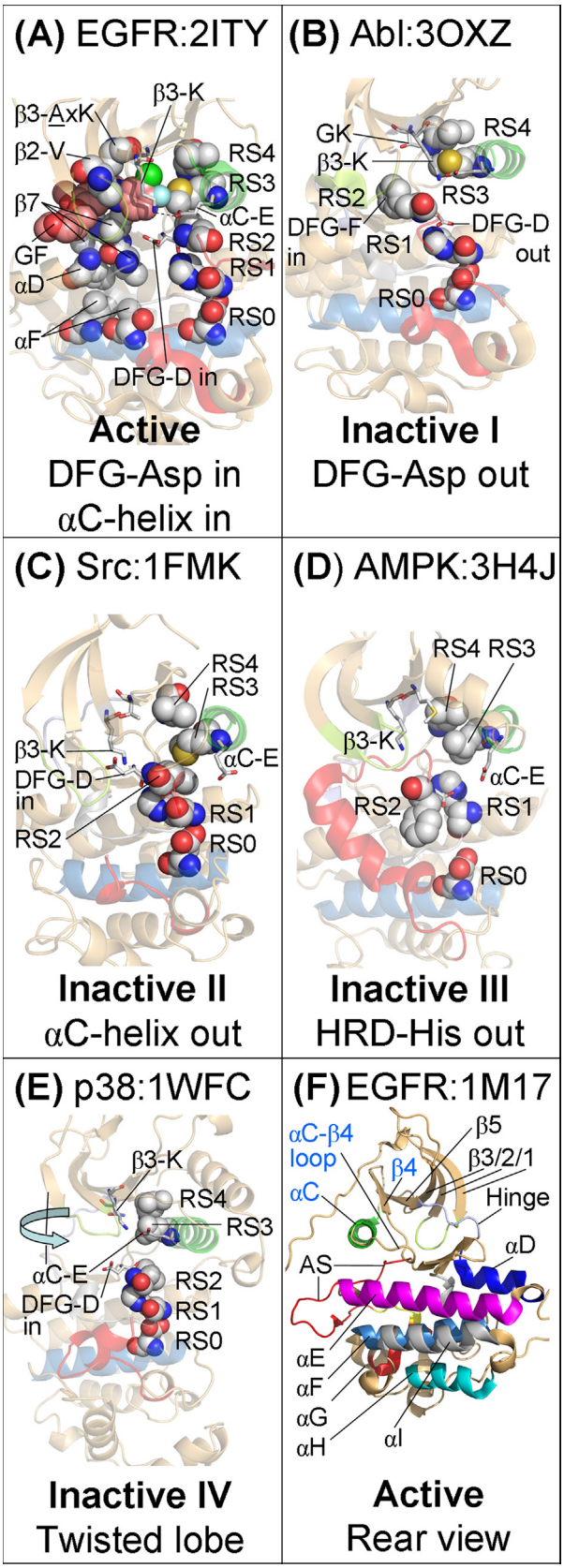

Fig. 2. (A) Frontal view of EGFR with its DFG-D in and αC-helix in active conformation. The space filling models on the left depict the C-spine and those on the right depict the R-spine. (B) Inactive I: DFG-Asp out. (C) Inactive II: αC-helix out. (D) Inactive III: HRD-His out. (E) Inactive IV: twisted lobe conformation. (F) Rear view of active EGFR to indicate the location of the αC-β4 or back loop residues that interact with many small molecule protein kinase antagonists. AS, activation segment; GF, gefitinib; RS, regulatory spine. All structures are human proteins except for D, which is from yeast. Classification of active and inactive forms adapted from Meharena et al. [10].

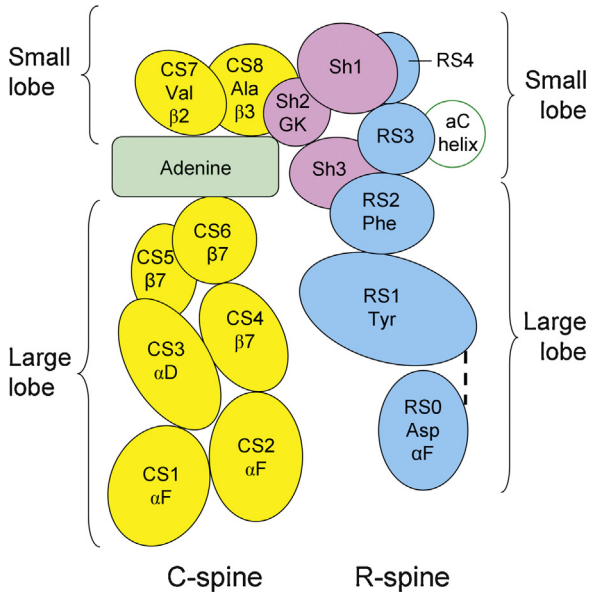

Fig. 3. Frontal view of the C- and R-spines of PKA. Note that RS1 in most protein kinases is histidine and not tyrosine [9]. The dashed line represents a hydrogen bond. Modeled after PDB ID: 1ATP. CS, C-spine; GK, gatekeeper; RS, R-spine; Sh, shell.

HRD-His out structure, the catalytic loop histidine (RS1) is separated from the aspartate of the αF-helix (RS0) (Fig. 2D). In the inactive twisted lobe structure, the N-lobe is rotated with an additional separation of the N-lobe (RS3) from the C-lobe (RS2) (Fig. 2E).

The catalytic spine of protein kinases consists of residues from the small amino-terminal and large carboxyterminal lobes that are completed by the adenine of ATP (Fig. 3) [10,16]. This spine mediates catalysis by facilitating ATP binding thereby accounting for the term catalytic. The two residues of the small lobe of protein kinase domains that bind to the adenine component of ATP include the alanine from the conserved Ala-Xxx-Lys of the β3-strand (CS8) and a hydrophobic valine residue from the beginning of the β2-strand (CS7) (Figs. 2A and 3). Furthermore, a hydrophobic residue from the middle of the β7-strand (CS6) binds to the adenine base in the active enzyme. This residue is flanked by two hydrophobic residues (CS4 and CS5) that bind to a residue near the beginning of the αD-helix (CS3). CS3 and CS4 interact with two residues of the αF-helix (CS1 and CS2) to complete the C-spine (Fig. 3). Using site-directed mutagenesis, Meharena et al. identified three residues in murine PKA that stabilize the R-spine that they labeled Sh1, Sh2, and Sh3, where Sh refers to shell [10]. The Sh2 residue corresponds to the gatekeeper residue. The name gatekeeper signifies the role that this residue plays in controlling access to the back cleft, which is described in Section 3.1. The back cleft is sometimes called the back pocket or hydrophobic pocket II (HPII).

Note that the αF-helix, which is entirely within the protein kinase domain, anchors both the R-spine and C-spine. Moreover, the spines in turn position the protein kinase catalytic residues. The residues that constitute the spines were identified by a comparison of the tertiary structure of 23 protein kinases in their active and inactive states based upon their X-ray crystallographic structures [15,16]. This contrasts with the identification of the DFG, APE, or HRD amino acid signatures based upon their primary structures [9].

Besides the hydrophobic interactions with the adenine group, the exocyclic 6-amino nitrogen of ATP characteristically forms a hydrogen bond with the carbonyl backbone residue of the first hinge residue that connects the small and large lobes of the protein kinase domain and the N1 nitrogen of the adenine base forms a second hydrogen bond with the N—H group

Table 2
Classification of small molecule protein kinase inhibitors.

Properties	Type I[a]	Type I1/2[c] (A/B)[b]	Type II[a] (A/B)[b]	Type III[a]	Type IV[d]	Type V[e]	Type VI
	Binds in the ATP-binding pocket of the active conformation	Binds in the ATP-binding pocket of an inactive DFG-Asp in conformation	Binds in the ATP-binding pocket of the inactive DFG-Asp out conformation	Allosteric inhibitor bound next to the ATP-site	Allosteric inhibitor not bound next to the ATP-site	Bivalent inhibitor spanning two regions	Covalent inhibitor
Extends into back cleft	No	(A) Yes/(B) no	(A) Yes/(B) no	Yes	No	Variable	Variable
DFG-Asp	In	In	Out	Variable	Variable	Variable	Variable
Activation segment	Out	Variable	Variable	Variable	Variable	Variable	Variable
αC	In	Variable	Variable	Out	Variable	Variable	Variable
Spine	Linear	Distorted	Usually distorted	Distorted	Variable	Variable	Variable
ATP-competitive	Yes	Yes	Yes	No	No	Variable	No
Reversible	Yes	Yes	Yes	Yes	Yes	Yes	Usually not

[a] Adapted from Dar and Shokat [18].
[b] A, drug extends into back cleft; B, drug does not extend into back cleft.
[c] Adapted from Zucotto et al. [20].
[d] Adapted from Gavrin and Saiah [21].
[e] Adapted from Lamba and Ghosh [22].

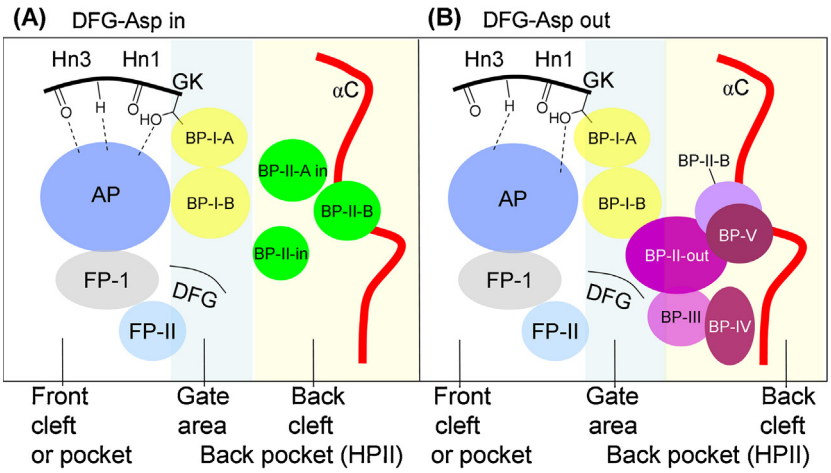

Fig. 4. Schematic overview of the binding pockets of the DFG-Asp in and DFG-Asp out protein kinase conformations. AP, adenine pocket; BP, back pocket; FP, front pocket; GK, gatekeeper; Hn, hinge; HP, hydrophobic. Adapted from van Linden et al. [24].

of third hinge residue. As noted later, most small-molecule inhibitors of protein kinases that are steady-state ATP competitive inhibitors also make hydrogen bonds with the backbone residues of the connecting hinge [17]. These antagonists also interact with residues that make up the C-spine, the R-spine, or both, and with other residues in various binding pockets as described later.

3. Classification of small molecule protein kinase inhibitors

3.1. Types of inhibitor

Dar and Shokat defined three classes of small molecule protein kinase inhibitor, which they labeled types I, II, and III [18]. They defined the type I inhibitor as "a small molecule that binds to the active conformation of a kinase in the ATP pocket," the type II inhibitor as "a small molecule that binds to an inactive (usually DFG-OUT) conformation of a kinase," and the type III inhibitor as "a non-ATP competitive inhibitor" or allosteric inhibitor. Allosteric ligands bind to a site distinct from the active site [19]; in the case of protein kinases, this refers to compounds that bind outside of the ATP-binding pocket. Zuccotto et al. introduced type I½ inhibitors as compounds that bind to "the adenine ring region like type I compounds establishing hydrogen bonds with the hinge region and then extend into the back cavity of the ATP site that give specific interactions with those residues that are involved with the type II pharmacophore" [20]. Thus the type I½ inhibitor binds to the protein kinases with the DFG-Asp in and αC-helix out conformation. Gavrin and Saiah divided allosteric effectors into two classes (III and IV) where the type III inhibitors bind within the cleft between the small and large lobes adjacent to the ATP binding pocket and type IV inhibitors bind outside of the cleft and the phosphoacceptor region [21]. Lamba and Gosh labeled bivalent molecules that span two regions of the protein kinase domain as type V inhibitors [22]. Small molecules that form covalent adducts with the target enzyme are a different class that we label as type VI inhibitors.

The classification described herein uses these parameters with further subdivisions and criteria (Table 2). Whereas Dar and Shokat and Zuccotto et al. are flexible in their criteria for type I inhibitors by stating that they do not require a specific conformation of key structural elements such as the αC-helix or the DFG-Asp conformations [18,20], we employ the criterion that type I inhibitors bind to the active conformation with DFG-Asp in, the αC-helix in, and with the R-spine in its active linear configuration. If the drug is bound to the active conformation, the inhibitor is classified as type I. However, if the drug is bound to an inactive conformation, we do not consider it to be a type I inhibitor. Liao [23] and van Linden et al. [24] divided the cleft between the small and large lobes into a front cleft, the gate area, and the back cleft. They also described several sub-pockets within these three regions, which are depicted in Fig. 4.

We have divided the type I½ and type II inhibitors into A and B subtypes. The binding of imatinib to Abl with the DFG-D out configuration while extending into the back cleft [25] was the first example of type II inhibition and we thereby classified imatinib and other drugs that extend into the back cleft as type A inhibitors. If the drug binds to the DFG-D out conformation while not extending into the back cleft, we classified these as type B inhibitors. The practical consequence of this distinction is that type A inhibitors may bind to the target kinase with a long residence time when compared with type B inhibitors as described in Section 9.

This paper describes the mode of action of FDA-approved small molecule protein kinase inhibitors as determined by X-ray crystallography. The chief targets of these drugs are listed in Table 3. The code for the drugs is a useful aid in searches of the early literature that may yield results that queries with the generic drug name misses. Unfortunately, crystal structures of several of the approved drugs with their protein kinase target are not available. Everolimus, sirolimus (rapamycin), and temsirolimus bind to FKBP12 (FK506-binding protein of 12 kDa). Each binary complex of drug and FKBP12 inhibits the protein-serine/threonine kinase mTOR (mammalian target of rapamycin), which belongs the phosphatidylinositol 3-kinase-related protein kinase family. Because these three drugs do not bind next to the ATP-binding pocket and are indirect inhibitors of protein kinase activity, they are classified as type IV allosteric inhibitors. The PI3K/AKT/mTOR pathway is activated by several receptor protein-tyrosine kinases including EGFR, ErbB3, c-Met, PDGFR, and VEGFR [27]. mTOR catalyzes the phosphorylation of several proteins that regulate protein translation as it promotes cell growth, apoptosis, and angiogenesis [28,29]. Each of these type IV inhibitors is used in the treatment of cancers (Table 3) while sirolimus also possesses immunosuppressive activity by inhibiting T-cell activation, proliferation, and antibody production. All of the drugs listed in Table 3 are orally effective except for temsirolimus, which is given by intravenous infusion.

Table 3
Classes of FDA-approved small molecule protein kinase inhibitors[a].

Name, code, trade name	Selected targets[b]	Indications[c]	Year approved	Company	Class[d]
Afatinib, Gilotrif, Tovok	EGFR, ErbB2/4	NSCLC	2013	Boehringer-Ingelheim	VI
Axitinib, AG013736, Inlyta	VEGFR1/2/3, PDGFRβ, Kit	RCC	2012	Pfizer	IIA
Bosutinib, SKI-606, Bosulif	BCR–Abl, Src, Lyn, Hck	Ph^+ CML	2012	Wyeth	I/IIB
Cabozantinib, XL184, BMS907351, Cometriq	RET, c-Met, VEGFR1/2/3, Kit, TrkB, Flt3, Axl, Tie2	Medullary thyroid carcinoma	2012	Exelexis	I
Ceritinib, LDK378, Zykadia	ALK, IGF-1R, InsR, ROS1	ALK^+ NSCLC after crizotinib resistance	2014	Novartis	I
Crizotinib, PF-02341066, Xalkori	ALK, c-Met (HGFR), ROS1, MST1R	ALK^+ NSCLC	2011	Pfizer	I/I½B
Dabrafenib, 6964, Tafinlar	B-Raf	Melanoma with *BRAF V600E* mutation	2013	GlaxoSmith-Kline	II
Dasatinib, BM-354825, Sprycel	BCR–Abl, Src, Lck, Lyn, Yes, Fyn, Kit, EphA2, PDGFRβ	Ph^+ CML, Ph^+ ALL	2006	GlaxoSmith-Kline	I/I½A
Erlotinib, OSI-744, Tarceva	EGFR	NSCLC, pancreatic cancer	2004	Roche, OSI	I/I½B
Everolimus, Rad001, Afinitor	FKBP12/mTOR	$HER2^-$ breast cancer, PNET, RCC, RAML, SEGA	2009	Novartis	IV
Gefitinib, ZD1839, Iressa	EGFR, PDGFR	NSCLC	2003	AstraZeneca	I
Ibrutinib, PCI-32765, Imbruvica	BTK	MCL, CLL, WM	2013	Janssen, Pharmacyclics	VI
Imatinib, STI571, Gleevec	BCR–Abl, Kit, PDGFR	Ph^+ CML, Ph^+ B-ALL, DFSP, GIST, HES, MDS/MPD, ASM	2001	Novartis	IIA
Lapatinib, GW2016, Tykerb	EGFR, ErbB2	Breast cancer	2007	GlaxoSmith-Kline	I/I½A
Lenvatinib, E7080, Lenvima	VEGFR1/2/3, FGFR1/2/3/4, PDGFRα, Kit, RET	DTC	2015	Eisai	I1/2A
Nilotinib, AMN107, Tasigna	BCR–Abl, PDGFR, DDR1	Ph^+ CML	2007	Novartis	IIA
Nintedanib, BIBF 1120, Ofev	FGFR1/2/3, Flt3, Lck, PDGFRα/β, VEGFR1/2/3	Idiopathic pulmonary fibrosis	2014	Boehringer-Ingelheim	IIB
Palbociclib, PD-0332991, Ibrance	CDK4/6	ER^+ and $HER2^-$ breast cancer	2015	Park Davis	I
Pazopanib, GW-786034, Votrient	VEGFR1/2/3, PDGFRα/β, FGFR1/3, Kit, Lck, Fms, Itk	RCC, soft tissue sarcoma	2009	GlaxoSmith-Kline	I
Ponatinib, AP24534, Iclusig	BCR–Abl, BCR–Abl T315I, VEGFR, PDGFR, FGFR, EphR, Src family kinases, Kit, RET, Tie2, Flt3	Ph^+ CML, Ph^+ALL	2012	Ariad	I
Regorafenib, BAY 73-4506, Stivarga	VEGFR1/2/3, BCR–Abl, B-Raf, B-Raf (V600E), Kit, PDGFRα/β, RET, FGFR1/2, Tie2, and Eph2A	CRC, GIST	2012	Bayer	IIA
Ruxolitinib, INC424, Jakafi	JAK1/2	Myelofibrosis, PV	2011	Incyte	I
Sirolimus, Rapamune	FKBP12/mTOR	Kidney transplants, lymphangioleiomyomatosis	1999	Wyeth	IV
Sorafenib, BAY 43-9006, Nexavar	B-Raf, CDK8, Kit, Flt3, RET, VEGFR1/2/3, PDGFR	HCC, RCC, DTC	2005	Bayer	IIA
Sunitinib, SU11248, Sutent	PDGFRα/β, VEGFR1/2/3, Kit, Flt3, CSF-1R, RET	RCC, GIST, PNET	2006	Pfizer	I½B/IIB
Temsirolimus, CCI-779, Torisel	FKBP12/mTOR	Advanced RCC	2007	Wyeth	IV
Tofacitinib, CP-690550, Xeljanz	JAK3	Rheumatoid arthritis	2012	Pfizer	I
Trametinib, 6495, Mekinist	MEK1/2	Melanoma with *BRAF V600E* mutations	2013	GlaxoSmith-Kline	III
Vandetanib, ZD6474, Caprelsa	EGFR, VEGFR, RET, Tie2, Brk, EphR	Medullary thyroid cancer	2011	AstraZeneca	I
Vemurafenib, PLX4043, Zelboraf	A/B/C-Raf and B-Raf (V600E)	Melanoma with *BRAF V600E* mutations	2011	Roche, Plexxicon	I½A

[a] ALL, acute lymphoblastic leukemia; ASM, aggressive systemic mastocytosis; CML, chronic myelogenous leukemia; CRC, colorectal cancer; DDR1, Discoidin domain receptor family, member 1; CLL, chronic lymphocytic leukemia; CML, chronic myelogenous leukemia; DFSP, dermatofibrosarcoma protuberans; DTC, differentiated thyroid carcinoma; ER, estrogen receptor; FKBP, FK506 (fujimycin) binding protein; GIST, gastrointestinal stromal tumor; HCC, hepatocellular carcinoma; HES, hypereosinophilic syndrome; IGF1-R, insulin-like growth factor-1 receptor; InsR, insulin receptor; MCL, mantle cell lymphoma; MDS/MPD, myelodysplastic/myeloproliferative diseases; MST1R or RON, macrophage stimulating protein receptor; NSCLC, non-small cell lung cancer; PNET, progressive neuroendocrine tumors of pancreatic origin; NSCLC, non-small cell lung cancer; PV, polycythemia vera; RAML, renal angiomyolipoma; RCC, renal cell carcinoma; SEGA, subependymal giant cell astrocytomas in tuberous sclerosis; WM, Waldenström's macroglobulinemia.
[b] Adapted from www.brimr.org/PKI/PKIs.htm and Fabbro et al. [26].
[c] See each FDA label for the precise indications.
[d] See text for a description of the various types of inhibitor.

3.2. A preview of the binding properties of inhibitors to protein kinase domains

The various classes of inhibitor are based upon the activation state of the protein kinase target. Specifically, the disposition of DFG-Asp (active in, inactive out), the αC-helix (active in, inactive out), and the regulatory spine (active linear, inactive distorted) is made. Except for type III allosteric inhibitors, all of the FDA-approved reversible inhibitors form hydrogen bonds with one or more hinge residues. Nearly all of the antagonists interact with a hydrophobic residue that occurs within the β1-strand immediately before the G-rich loop. Most of the inhibitors form hydrophobic contacts with catalytic spine residues CS6, CS7, and CS8 that occur within the (i) β7-strand, (ii) β2-strand, and (iii) β3-strand, respectively (Figs. 2A and 3). Many inhibitors also make hydrophobic contacts with the aliphatic side chain of the β3-strand lysine residue (the K of K/E/D/D). About half of the inhibitors interact (i) with the RS3 R-spine residue within the αC-helix, and (ii) with the gatekeeper residue. Interactions with the gatekeeper may involve hydrogen-bonding or they may be hydrophobic in nature. About

two-thirds of the inhibitors interact with one or more residues in the αC-β4 or back loop,

Most of the FDA-approved inhibitors make a hydrophobic contact with residues that occur just before the DFG-D of the activation segment. Hydrophobic interactions with the DFG-F are also common. Nearly all of the inhibitors interact with the DFG-D at the beginning of the activation segment; these contacts vary and may involve hydrogen bonds, salt bridges, hydrophobic interactions, and van der Waals forces. That the adenine of ATP forms part of the C-spine and the small molecule inhibitors also bind within the adenine pocket accounts in large part for the interaction of these antagonists with the catalytic spine residue within the β2-, β3-, and β7-strands. The following section characterizes the binding of FDA-approved inhibitors to their various drug targets and their interaction with regions of the protein kinase domain that are specific for each protein kinase target.

4. Type I inhibitors

Table 4 includes ten FDA-approved small molecule protein kinase type I inhibitors that have been demonstrated to bind to the active form of their protein kinase target. Dysregulation of EGFR protein-tyrosine kinase activity has been implicated in the oncogenic transformation of various types of cells and represents an important drug target [30–32]. For example, amplification or activation of EGFR has been observed in NSCLC. An L858R or a G719S mutation or small in-frame deletions of exon 19 corresponding to the regulatory αC-helix lead to the expression of activated EGFRs in NSCLC that are sensitive to gefitinib and erlotinib [33]. These were two of the earliest small molecule protein kinase inhibitors that were approved by the FDA and they are used for the treatment of NSCLC. Gefitinib is prescribed for the treatment of patients bearing exon 19 deletions or the activating exon21 L858R mutation and erlotinib is used as a second-line treatment for patients that have undergone a cytotoxic treatment regimen. Erlotinib is also approved for the first-line treatment of pancreatic cancer. Lapatinib is a type I½A inhibitor while afatinib is an irreversible EGFR inhibitor, both of which are FDA-approved (Table 3). All four of these EGFR antagonists bear a quinazoline scaffold that occupies the adenine pocket, a 4-amino substituent that binds in a hydrophobic pocket within the gate area while a long chain from the 6-position, the 7-position, or both (Fig. 5E, F, K, and V) extend toward the solvent and increase the overall water solubility of the drug.

Gefitinib is a type I inhibitor of EGFR. The X-ray structure indicates that the quinazoline N1 nitrogen makes one hydrogen bond with the N—H group of M793 of the hinge (Fig. 6A) [34]. Its 3-chloro-4-fluoro-phenyl group makes hydrophobic contacts with residues in the gate area. The aniline ring forms a 45° angle with the plane of the quinazoline and the chloro group is directed upward. The methoxy group in the 7 position of the quinazoline is in van der Waals contact with G796 while the 6-propylmorpholino group extends into the solvent. Overall the drug makes hydrophobic contacts with the β1-strand L718 before the G-rich loop, the β2 C-spine V726 (CS7), the β3 C-spine A743 (CS8) and K745, the RS3 M766 of the R-spine, β5 L788, the gatekeeper T790, and ^{791}QLMP^{794} of the hinge, the β7-strand C-spine L844 (CS6), and the drug makes van der Waals contact with DFG-D855 of the activation segment (not shown). Gefitinib was initially approved by the FDA in 2003, but its approval was withdrawn in 2005 only to be reinstated in 2015. Early work by Ciardiello et al. indicated that the addition of cytotoxic paclitaxel or carboplatin to gefitinib led to decreased proliferation of human ovarian cells in culture [35]. However, Ellis et al. reported that the addition of these agents to gefitinib has not proven advantageous in the treatment of NSCLC [36].

Erlotinib is a type I and type I½B inhibitor of EGFR that is approved for the treatment of NSCLC and pancreatic cancer. As a type I inhibitor, the N1 nitrogen of the erlotinib quinazoline makes one hydrogen bond with the EGFR M793 N—H group of the hinge (Fig. 6B) [37]. The N3 nitrogen is not within hydrogen bonding distance with the T790 gatekeeper (4.1 Å), but a water molecule bridges this gap. The interplaner angle of the aromatic ring systems is 42°. The 3-ethynylphenyl group of the drug makes hydrophobic contacts with residues within the gatekeeper area. Overall the drug makes hydrophobic contacts with the β1-strand L718, CS8 A743, the β3 K745, L788 of the β5-strand, the gatekeeper T790, and ^{791}QLMPF^{795} of the hinge, CS6 L844, T854 before the activation segment, and the drug makes van der Waals contact with DFG-D855. The proximal 2-methoxyethoxy groups project toward the solvent. The drug-free protein kinase domain and the erlotinib-EGFR complex are superimposable with RMS deviations of only 0.4 Å [37]. Neither gefitinib nor erlotinib occupies the back cleft. They have comparable inhibitor profiles and their binding to EGFR as a type I inhibitor in these two cases is similar. Erlotinib is used in patients with NSCLC that have received platinum-based first-line chemotherapy. Clinical studies indicate that there is no benefit for the addition of erlotinib to first-line platinum-based chemotherapy [36]. Although erlotinib is approved for the treatment of pancreatic cancer, this is one of the most lethal forms of cancer and its benefits are marginal [38].

Rowley discovered that the Philadelphia chromosome is formed from a reciprocal translocation t(9;22)(q34;q11.2) that results in a lengthened chromosome 9 and a shortened chromosome 22 (the Philadelphia chromosome) [39]. The Philadelphia chromosome occurs in about 95% of CML patients and about 25% of patients with ALL (acute lymphoblastic leukemia). The BCR–Abl oncogene results from this translocation [5,40]. As a result, the physiological N-terminal inhibitory domain of Abl is eliminated thereby leading to an activated BCR–Abl kinase, which stimulates multiple signaling pathways and is the major factor in the pathogenesis of these diseases. Imatinib was the first medication approved for the treatment of Ph$^+$ CML, but resistance to the imatinib prompted the development of second-generation inhibitors such as dasatinib and bosutinib [41].

Dasatinib is a type I inhibitor of Abl that is approved for the treatment of Ph$^+$ imatinib-resistant (i) CML and (ii) ALL; it can also be used as a first-line treatment for newly diagnosed Ph$^+$ CML. The aminothiazole group occupies the adenine pocket [42]. The N3 nitrogen of the thiazole scaffold forms one hydrogen bond with the N—H group of the Abl M318 hinge and the amino group linking the thiazole with the pyrimidine ring of dasatinib forms a hydrogen bond with the Abl M318 carbonyl group of the hinge. The distal toluidine group points toward the front cleft hydrophobic pocket FP-I close to the Thr315 gatekeeper and the connecting amide N—H forms a hydrogen bond with the gatekeeper T315 (Fig. 6C). Accordingly, T315I mutation-related drug resistance also occurs in patients treated with dasatinib. The distal 2-chloro-6-methyl phenyl ring of dasatinib is orthogonal to the thiazole carboxamide group and the proximal piperazine group is directed toward the solvent. On the whole the drug makes hydrophobic contacts with the β1-strand L248 before the G-rich loop, Y253 within the loop, CS7 A269, V270 and K271 of the β3-strand, RS3 M290, V299 of the αC-β4 or back loop, I313 of the β5-strand, ^{317}FMTY^{320} of the hinge, CS6 L370, and A330 just before the DFG-D331. The αC-E286 carboxylate makes a hydrogen bond with the β3-K271 ϵ-amino group and another with the N—H group of RS2 DFG-F382 (Fig. 6C).

Dasatinib is 300-fold more potent than imatinib based upon studies with purified Abl and against cells expressing BCR–Abl [43]. It is effective against the more common imatinib-resistant mutations with the exception of that of the important T315I gatekeeper. Dasatinib is a multikinase inhibitor that targets several protein

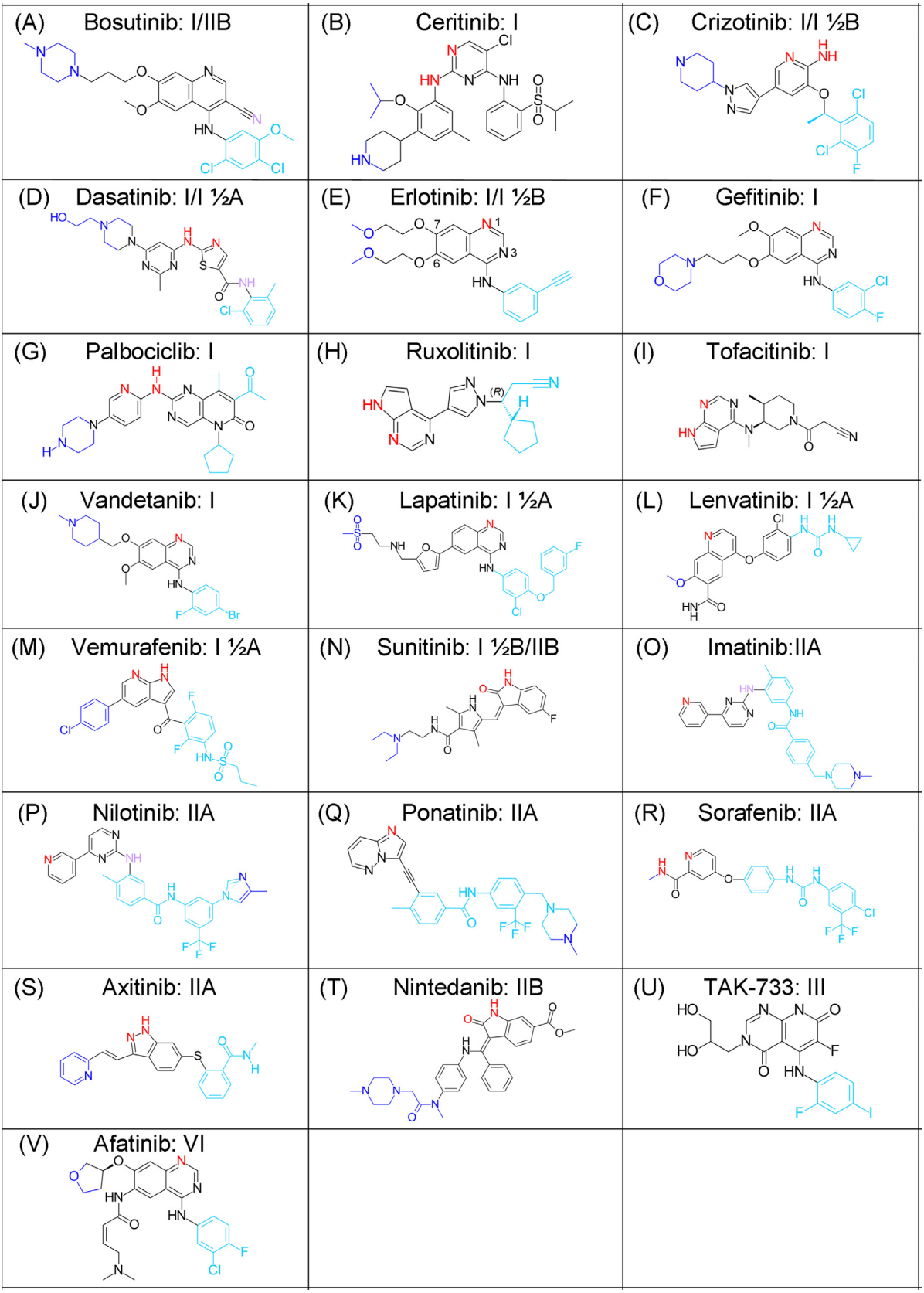

Fig. 5. Chemical structures and classification of small molecule protein kinase inhibitors. All of these are FDA-approved except for TAK-733. Atoms that make hydrogen bonds with the hinge are colored red and those that make hydrogen bonds with a gatekeeper are colored purple. The dark-blue colored atoms extend out of the kinase domain into the solvent and the sky-blue colored atoms interact with hydrophobic pockets. Adapted from Ref. [24]. For the chemical structures of all FDA-approved small molecule protein kinase inhibitors see www.brimr.org/PKI/PKIs.htm.

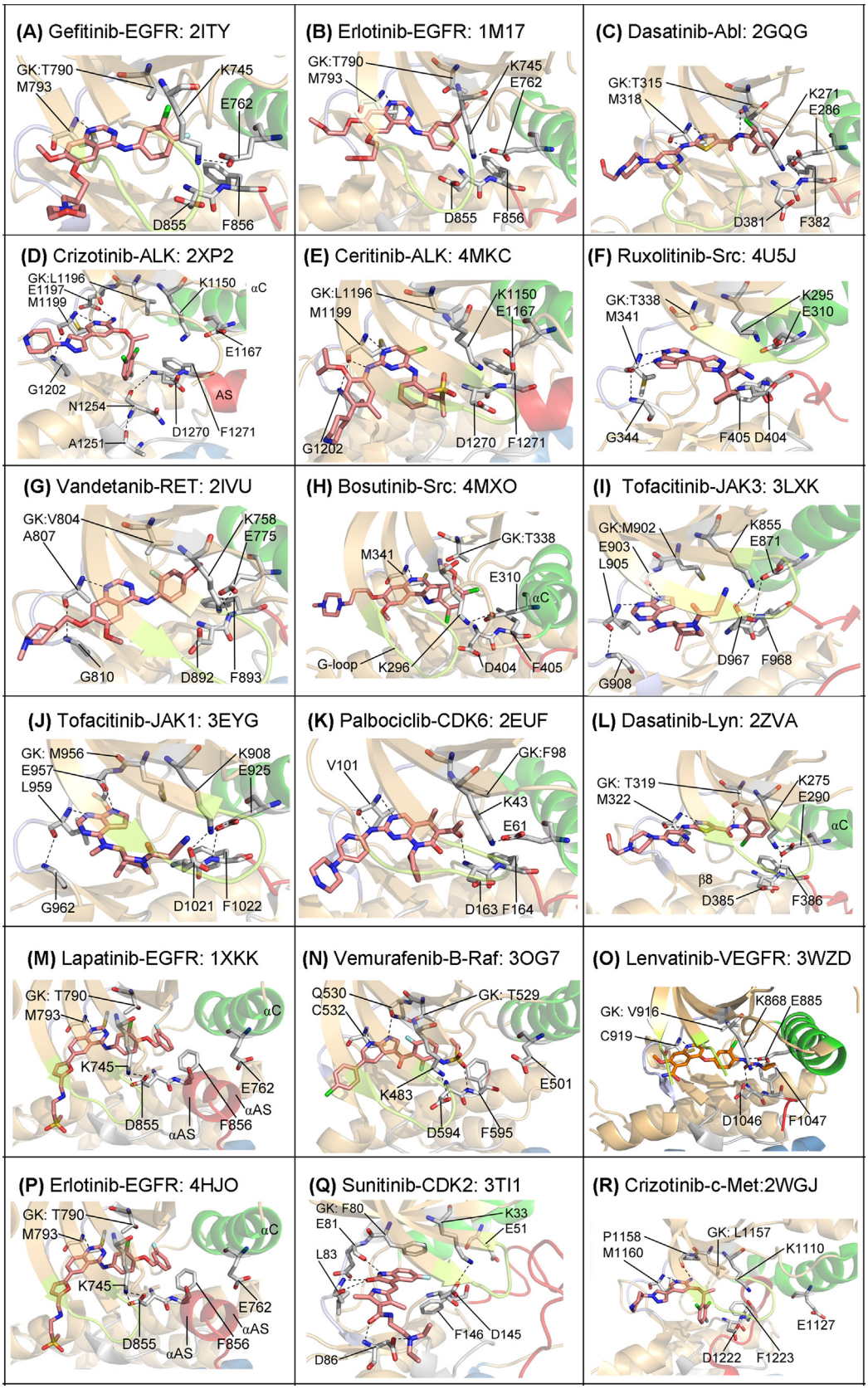

Fig. 6. Type I, I½A, and I½B inhibitors. The protein kinase and corresponding PDB ID of each drug-enzyme complex are listed. The drug carbon atoms are orange and those of the enzyme are gray. The dashed lines represent polar bonds. The EGFR residue numbers of PDB ID: 1M17 (4B) and 4HJO (4P) lack the signal sequence [30], but these 24 residues were included here to be consistent with other EGFR depictions. AS, activation segment; αAS, an α-helix near the origin of the activation segment; GK, gatekeeper.

Table 4
Drug-protein kinase interactions.

Drug-enzyme[a]	PDB ID	DFG-D	AS[b]	αC	R-Spine	GK[c]	Inhibitor class	Pockets and sub-pockets occupied[d]
Bosutinib-Src	4MXO	In	Open	In	Active	T	I	F, G, BP-I-A/B
Ceritinib-ALK	4MKC	In	Open	In	Active	L	I	F, FP-I
Crizotinib-ALK	2XP2	In	Open	In	Active	L	I	F, FP-I
Dasatinib-Abl	2GQG	In	Open	In	Active	T	I	F, FP-I
Erlotinib-EGFR	1M17	In	Open	In	Active	T	I	F, G, BP-I-A/B
Gefitinib-EGFR	2ITY	In	Open	In	Active	T	I	F, G, BP-I-A/B
Palbociclib-CDK6	2EUF	In	Open	In	Active	F	I	F
Ruxolitinib-Src[e]	4U5J	In	Open	In	Active	T	I	F[g]
Tofacitinib-JAK3	3LXK	In	Open	In	Active	M	I	F, FP-I/II
Tofacitinib-JAK1	3EYG	In	Open	In	Active	M	I	F, FP-I/II
Vandetanib-RET	2IVU	In	Open	In	Active	V	I	F, G, BP-I-A/B
Dasatinib-Lyn[f]	2ZVA	In	Open	In	RS2/3/4 up	T	I ½ A	F, G, B, BP-I-A/B
Lapatinib-EGFR	1XKK	In	Closed	out	RS2/3→	T	I ½ A	F, G, B, BP-I-A/B, II in, IIA in
Lenvatinib-VEGFR	3WZD	In	?	In	RS3/4 up	V	I ½ A	F, G, B, IB, II in
Vemurafenib-B-Raf	3OG7	In	?	out	RS3→	T	I ½ A	F, G, B
Crizotinib-Met	2WGJ	In	Closed	out	←RS4	L	I ½ B	F, FP-I
Erlotinib-EGFR	4HJO	In	Closed	out	RS2/3→	T	I ½ B	F, G, BP-I-A/B
Sunitinib- CDK2	3TI1	In	Closed	out	RS3→	F	I ½ B	F
Axitinib-VEGFR	4AG8	Out	Closed	In	←RS2/4	V	IIA	F, G, B, BP-I-B, II out
Imatinib-Abl[f]	1IEP	Out	Closed	In	←RS2	T	IIA	F, G, B, BP-I-A/B, II out, IV
Imatinib-Kit	1T46	Out	Closed	In	←RS2	T	IIA	F, G, B, BP-I-A/B, II out, IV
Nilotinib-Abl	3CS9	Out	Closed	In	←RS2	T	IIA	F, G, B, BP-I-A/B, II out, III,V
Ponatinib-Abl[f]	3OXZ	Out	Closed	In	←RS2	T	IIA	F, G, B, BP-I-A/B, II out, III,IV
Ponatinib-Kit	4U0I	Out	Closed	In	←RS2	T	IIA	F, G, B, BP-I-A/B, II out, III,IV
Ponatinib-B-Raf	1UWH	Out	?	In	←RS2/4	T	IIA	F, G, B, BP-I-B, II out, III
Sorafenib-CDK8	3RGF	Out	?	In	←RS2/4	F	IIA	F, G, B, BP-I-B, II out, III
Sorafenib-VEGFR	4ASD	Out	Closed	In	←RS2	V	IIA	F, G, B, BP-I-B, II-out, III
Bosutinib-Abl	3UE4	Out	Open	In	←RS2	T	IIB	F, G, BP-I-A/B
Nintedanib-VEGFR2	3C7Q	Out	Closed	In	←RS2	V	IIB	F, G, BP-I-B
Sunitinib-Kit	3G0E	Out	Closed	In	←RS2	T	IIB	F
Sunitinib-VEGFR	4AGD	Out	Closed	In	←RS2	V	IIB	F, BP-I-B
TAK-733-MEK1	3PP1	In	Closed	Out	RS3/4→	M	III	G, B, BP-II in
Afatinib-EGFR	4G5J	In	Open	In	Active	T	VI	F, G, BP-I-A/B[g]

[a] All human proteins unless otherwise noted.
[b] Activation segment.
[c] Gatekeeper residue.
[d] F, front cleft; G, gate area; B, back cleft; from http://klifs.vu-compmedchem.nl/ unless otherwise noted. F, G, and B are the pockets.
[e] Chicken enzyme.
[f] Mouse enzyme.
[g] Inferred.

kinases including those of the Src family (Table 3) and its therapeutic efficacy may involve inhibition of protein kinases in addition to Abl [44]. A higher proportion of patients treated with dasatinib exhibit lower peripheral blood BCR–Abl transcript levels as determined by real-time quantitative PCR when compared with dasatinib [45]. However, dasatinib patients experience more grade 3–4 toxicities when compared with imatinib. Dasatinib, imatinib, and nilotinib are equally effective as first-line treatments for CML, but ongoing clinical studies continue to compare and optimize their effectiveness [45].

Anaplastic lymphoma kinase is a member of the insulin receptor protein-tyrosine kinase superfamily [46]. It was initially described in an anaplastic large cell lymphoma, but it has been shown to participate in other neoplastic disorders including sporadic and hereditary neuroblastomas and renal cell carcinomas [47,48]. Soda et al. [49] and Rickova et al. [50] characterized an EML4 (echinoderm microtubule-associated protein like 4)-ALK oncoprotein that occurs in about 5% of NSCLC patients. Owing to the widespread prevalence of NSCLC, ALK became an important target for drug discovery. The incidence of ALK^+ NSCLC in the United States per year (11,000) is about twice that of CML (6700). Crizotinib was the first medication approved for the treatment of ALK^+ NSCLC (Table 3).

Crizotinib is a type I inhibitor of ALK and is approved for the first line treatment of ALK^+ NSCLC. The amino group of the aminopyrimidine scaffold of crizotinib (Fig. 5C) makes one hydrogen bond with the carbonyl group of ALK E1197 (the first hinge residue), the N1 nitrogen of the pyrimidine makes another with the N—H group of M1199 (the third hinge residue), and the carbonyl group of M1199 makes a hydrogen bond with G1202 (the sixth hinge residue) (Fig. 6D). The 2, 6-dichloro-3-fluorophenyl group interacts with FP-I in the front cleft. Overall crizotinib makes hydrophobic contacts with L1122 within the G-rich loop, CS7 V1130 after the loop, CS8 A1148, the gatekeeper L1196, ^{1198}LMA^{1200} of the hinge, R1253 and N1254 of the catalytic loop, CS6 L1256, and DFG-D1270. The proximal piperidine ring, which is attached to the N1 position of the pyrazol-4-yl, is directed toward the solvent. The carbonyl group of N1254 of the catalytic loop makes a hydrogen bond with the N—H group of DFG-D1270 and the carbonyl group of A1251 also within the catalytic loop makes a hydrogen bond with the N—H group of the catalytic loop N1254 (Fig. 6D). Crizotinib targets additional protein kinases including the c-MET proto-oncogene-encoded protein-tyrosine kinase, which corresponds to the hepatocyte growth factor receptor (HGFR) (its original drug target [47,51], and the ROS proto-oncogene 1-encoded kinase (ROS1) of the tyrosine kinase insulin receptor class [52]).

Resistance to crizotinib in the treatment of NSCLC occurs with a median duration of 10.5 months [53]. Mutations and the overexpression of ALK fusion proteins account for about one-third of crizotinib resistance, up-regulation or the overexpression of ALK fusion proteins account for another third, and up-regulation of alternative signaling pathways accounts for the remainder. The most common ALK mutation that confers crizotinib resistance is

the L1196M gatekeeper mutation and other resistance mutations include G1269A, I1171T, S1206Y, G1202R, and F1174C mutations [54]. The gatekeeper L1196M and hinge G1269A mutation sterically block crizotinib binding [55]. Such drug-resistant mutations prompted the development of second generation ALK inhibitors such as ceritinib. This drug is approved by the FDA for the treatment ALK^+ NSCLC in patients who have progressed on or are intolerant to crizotinib. Ceritinib overcomes ALK bearing L1196M, G1269A, I1171T, and S1206Y mutations, but not ALK with G1202R and F1174C mutations [55].

Ceritinib is a type I inhibitor of ALK and the crystal structure depicts a binding mode similar to that of the ALK–crizotinib complex with the DFG-Asp in conformation [55]. The 2, 4-diaminopyrimidine scaffold of the drug (Fig. 5B) forms two hydrogen bonds with M1199 of the ALK hinge (Fig. 6E). β3-K1150 forms a hydrogen bond with a water molecule that in turn binds to one of the sulfonyl oxygens (not shown). The isopropylsulfonylphenyl group occupies the hydrophobic FP-I within the front cleft. Ceritinib makes hydrophobic contacts with the β1-strand L1122, CS7 V1130 after the G-rich loop, CS8 A1148, β3-K1150, the gatekeeper L1196, ^{1198}LMA^{1200} of the hinge, and CS6 L1256. The anchor-shaped terminal 2-isopropoxy-3-(piperidin-4-yl) phenyl group lies in the interface between the solvent and the ATP-binding pocket. Ceritinib inhibits the insulin like growth factor-1 receptor, the insulin receptor, and ROS1 protein kinases with an inhibitor profile that partially overlaps that of crizotinib. Crizotinib and ceritinib bind to ALK in a similar fashion and neither occupies the back cleft. As noted above, ceritinib is effective against the L1196 M gatekeeper mutant of ALK whereas crizotinib is not.

Ruxolitinib is a type I inhibitor of JAK1/2 that is approved for the treatment of polycythemia vera and primary myelofibrosis. The Janus kinase family of intracellular protein-tyrosine kinases consists of four members: JAK1/2/3 and Tyk2. JAK1 plays a major role in the signaling of a number of proinflammatory cytokines and JAK2 interacts with receptors for hematopoietic growth factors such as erythropoietin and thrombopoietin [56]. JAK3 plays a primary role in mediating immune function and Tyk2 participates in interferon-α signaling. These proteins contain an N-terminal FERM domain, two SH2-like domains, an inactive pseudokinase domain, and finally an active protein kinase domain. The pseudokinase domain ordinarily inhibits the functional N-terminal protein kinase domain. Janus is a two-faced Roman God of beginnings and endings, and the term was applied to this enzyme family owing to the presence of the two protein kinase domains within a single polypeptide chain.

Polycythemia vera is an illness characterized by excessive red blood cell production. This bone marrow neoplasm may also result in the overproduction of leukocytes and platelets. More than 95% of these individuals possess a JAK2 V617F mutation in the pseudokinase domain that obliterates its negative regulatory role on the functional kinase domain resulting in a constitutively active enzyme [57]. These patients are treated primarily with therapeutic phlebotomies to maintain a normal hematocrit and hydroxyurea (a ribonucleotide reductase antagonist that decreases the production of deoxyribonucleotides); ruxolitinib represents a second-line treatment that is undergoing further clinical evaluation to optimize its use in polycythemia vera [57]. Primary myelofibrosis is a myeloproliferative neoplasm that is characterized by the deposition of scar tissue in the bone marrow; about half of the affected people possess the JAK2 V617F mutation. Ruxolitinib is used as a first-line treatment for these individuals.

Duan et al. [58] determined the crystal structure of ruxolitinib bound to Src and determined that it is a type I inhibitor. They docked ruxolitinib into the binding pocket of a previously solved JAK1 kinase and their results suggested that the drug also binds to this enzyme as a type I inhibitor. The drug is oriented such that the pyrrolopyrimidine ring (Fig. 5H) points toward the Src hinge region, the cyclopentane ring is directed toward the C-lobe, while the propanenitrile group points toward G276, the second glycine of the G-rich loop. The N1 nitrogen of the pyrrolopyrimidine platform of ruxolitinib serves as a hydrogen-bond acceptor with the N—H group of the Src hinge M341 and the N7 N—H group of the platform serves as a hydrogen-bond donor with the M341 carbonyl group (Fig. 6F). The N3 nitrogen of the platform hydrogen bonds with a water molecule that makes a polar contact with the gatekeeper T338 (not shown). The cyclopentyl and propanenitrile groups of ruxolitinib make hydrophobic contacts with residues in the front cleft. Overall the drug makes hydrophobic contacts with the β1-strand L273 before the G-rich loop, CS7 V281, CS8 A293, Y340 and M341 of the hinge, A390 and N391 of the catalytic loop, CS6 L393, A403 just before the activation segment, and DFG-D404 of the activation segment. Ruxolitinib is one of the smaller protein kinase antagonists (MW 306) and it occupies only the front cleft of Src.

Vandetanib, which is an inhibitor of RET and EGFR, is approved for the treatment of medullary thyroid carcinomas. RET (rearranged during transfection) is a receptor protein-tyrosine kinase that responds to the glial-cell line derived neurotrophic family of ligands. RET consists of four cadherin-like domains (CLD1/2/3/4), a cysteine-rich domain (CRD), a transmembrane segment, a juxtamembrane segment, a tyrosyl kinase domain, and ends with a C-terminal tail [59]. RET loss-of-function mutations occur in Hirschsprung disease, which is characterized by the lack of neuronal ganglion cells in the colon. Activating RET mutations are found in several neoplasms including familial medullary thyroid carcinomas, multiple endocrine neoplasia-2A/2B, pheochromocytoma, and parathyroid hyperplasia. Activating RET mutations are also found in almost all cases of hereditary medullary thyroid carcinomas and in about 50% of cases of the sporadic disease [60].

Gain-of-function mutations are associated with the extracellular cysteine-rich domain and the intracellular protein kinase domain [59]. Activating mutations within the RET kinase domain are variable. A range of mutations such as L790F, Y791F, S891A, and R844L produce a moderately transforming RET that is found in medullary thyroid cancer and multiple endocrine neoplasia-2A/2B phenotypes. In contrast, the M918T mutation has a very high transforming ability and is found in 95% of multiple endocrine neoplasia-2B patients. The multiple endocrine neoplasia-2B phenotype involves not only the thyroid and adrenal glands, but it also involves a variety of mucosal, ocular, and skeletal abnormalities. In addition, the RET M918T mutant targets unique substrates such as STAT3 that may contribute to cell transformation. Besides mutations within the *RET* gene, chromosomal translocations can produce oncogenic fusion proteins such as RET/PTC that give rise to papillary thyroid cancer. RET/PTC fusion proteins are cytosolic and contain the RET kinase domain extending from E713 (exon 12) to the C-terminus. In many cases, the N-terminal domain of RET/PTC is a dimerization domain derived from the fusion partner. However, mutation of the residue in RET/PTC corresponding to Y905 of wild-type RET leads to reduced transforming ability. The loss-of-function or gain-of-function of many, but not all mutations, of the kinase domain can be rationalized based upon their location [59].

Early stage medullary thyroid cancer can be cured surgically. For unresectable locally advanced or metastatic disease, vandetanib represents a possible therapeutic option. Vandetanib is a type I inhibitor of RET that binds to the front cleft while the 4-bromo-2-fluorophenyl group (Fig. 5J) forms hydrophobic contacts within the gate area. The N1 nitrogen of the quinazoline group of the drug makes a hydrogen bond with the N—H group of A807 of the hinge. Moreover, the β3-K758 makes salt bridges with αC-E775 and DFG-D892 while αC-E775 forms a hydrogen bond with the N—H group of RS2 DFG-F893 (Fig. 6G) [59]. Overall vandetanib makes hydrophobic contacts with L730 of the G-rich loop, the β3 (i) CS8 A756, (ii)

V757, and (iii) K758, αC-E775, RS3 L779, L802 of the β5-strand, the gatekeeper V804, Y806 and A807 of the hinge, RS1 HRD-H872 and N879 of the catalytic loop, and CS6 L881. Furthermore, the drug makes van der Waals contact with DFG-D892. Vandetanib targets a few other protein kinases including EGFR and VEGFR (Table 3). Besides inhibiting RET, the inhibition of EGFR appears to play an import role in its action in medullary thyroid cancer by decreasing the production of angiogenic growth factors [61].

Bosutinib is another second-generation inhibitor used as a second-line treatment for imatinib-resistant CML. It is a type I inhibitor of Src and type IIB inhibitor of Abl. Bosutinib contains an anilinequinoline core that is similar to the anilinequinazoline core of several EGFR antagonists (Fig. 5A). In the case of Src, the N1 of the bosutinib quinoline group serves as a hydrogen bond acceptor with the N—H group of M341 within the hinge (Fig. 6H). The nitrile group of bosutinib extends into the gate area hydrophobic pocket BP-I-A near the Thr315 gatekeeper [62] and its substituted aniline group occupies the gate area hydrophobic pocket BP-I-B. We will see that this pattern is similar to that observed in the binding of bosutinib to Abl. In general the drug also makes hydrophobic contacts with the β1-strand L273, CS7 V281 after the G-rich loop, CS8 A293, the β3-strand I294 and K295, the RS3 M314 of the R-spine, V323 of the αC-β4 loop, the gatekeeper T338, Y340 and M341 of the hinge, and CS6 L393. The drug also makes van der Waals contact with DFG-D404. The bosutinib-Src complex is in the active αC-in conformation leaving the back cleft and its sub-pockets unoccupied. Bosutinib also targets Src family protein kinases (Table 3). However, the drug is not an effective antagonist of the Abl T315I gatekeeper mutant.

Tofacitinib is a type I inhibitor of the non-receptor protein-tyrosine kinase JAK3 and is approved for the treatment of rheumatoid arthritis. As noted for ruxolitinib above, the Janus kinase family participates in many aspects of cytokine and inflammatory signaling pathways. Like ruxolitinib, tofacitinib bears a pyrrolo[2,3-*d*]pyrimidine scaffold (Fig. 5I). X-ray crystal structures of complexes of tofacitinib with JAK1, JAK2, and JAK3 have been reported [63,64]. Tofacitinib binds within the adenine pocket of these proteins. The N7 N—H of the pyrrolo[2,3-*d*]pyrimidine scaffold forms one hydrogen bond with the hinge residue carbonyl group of Glu903 and the N1 nitrogen of the scaffold forms a second hydrogen bond with the N—H group of Leu905 in JAK3 (Glu 930 and Leu932 in JAK2; PDB ID: 3FUP and Glu979 and Val981 in Tyk2; PDB ID: 3LXN). A hydrogen bond is observed between (i) the hinge residues L905 and G908, (ii) β3-K855 and αC-E871, (iii) β3-K855 and DFG-D967, and (iv) αC-E871 and DFG-D967 (Fig. 6I). The terminal cyanoacetyl handle extends into the front cleft underneath the G-rich loop and the methyl group of the piperidine ring is also found within the front cleft. On the whole, tofacitinib makes hydrophobic contacts with the β1-strand L828 before the G-rich loop, CS7 V836, CS8 A853, V884 within the back loop, and M902, Y904, and L905 of the hinge, CS6 L956, and A966 just before the activation segment.

Tofacitinib binds to JAK1 in a fashion similar to that of JAK3. The drug is oriented such that the pyrrolopyrimidine ring points toward the hinge, the methyl group points toward the solvent, the piperidine ring is located in a polar pocket that involves β3-K908 and DFG-D1021 with its methyl group pointing toward the C-terminal lobe and the nitrile group is buried beneath the tip of the glycine loop. The N7 N—H of the pyrrolo[2,3-*d*]pyrimidine platform forms one hydrogen bond with the hinge residue carbonyl group of E957 and the N1 nitrogen of the platform forms a second hydrogen bond with the hinge residue N—H group of L959 in JAK1. A hydrogen bond is observed between (i) the hinge residues L959 and G962, (ii) β3-K908 and αC-E925, (iii) β3-K908 and the carbonyl group of DFG-D1021, and (iv) αC-E925 and the N—H group of DFG-F1022 (Fig. 6J) [64]. A large number of van der Waals interactions promote inhibitor binding. The drug makes hydrophobic contacts with L881 within the β1-strand before the G-rich loop, CS7 V889 after the loop, the β3-strand CS8 A906 and K908, the gatekeeper M956, F958 and L959 of the hinge, and L1010 after the catalytic loop. The efficacy of tofacitinib has been hindered by side effects such as anemia and neutropenia, probably due to undesirable inhibition of the entire JAK family; thus, it was not approved by European regulatory agencies.

Palbociclib is a type I inhibitor of CDK4/6 that is approved for the treatment of estrogen receptor-positive and HER2-negative breast cancer. Cyclin-dependent kinases (CDKs) are a family of 20 protein-serine/threonine kinases first discovered for their role in regulating the cell cycle and then in regulating protein translation; thus, they represent a natural anticancer target [65,66]. These enzymes are activated by various cyclins. For example, CDK4 and CDK6 are activated by cyclin D, which promotes G1/S cell cycle progression. The scaffold of palbociclib consists of a pyrido[2,3-*d*]pyrimidinone core (Fig. 5G). The crystal structure of palbociclib with CDK6 shows that one hydrogen bond forms between the carbonyl group of Val101 of the hinge and the 2-amino group attached to the pyridopyrimidine core. Another hydrogen bond forms between the N3 nitrogen of the core and the N—H group of Val101 and a third hydrogen bond is formed between the DFG-D163 N—H group and the 6-acetyl carbonyl group (Fig. 6K) [67]. The 5-methyl and 6-acetyl groups occupy hydrophobic pocket BP-I-A in the gate area. The piperazinylpyridinylamino substituent at the 2-position of the pyrido[2,3-*d*]pyrimidinone core faces the solvent. On the whole, palbociclib makes hydrophobic contacts with the β1-strand I19, CS7 V27, β3-K43, V77 within the αC-β4 loop, the F98 gatekeeper, Q103 of the hinge, CS6 L152, and A162, which occurs just before the activation segment. The cyclopentyl group occurs close to where the ribose of ATP is expected to bind. The addition of palbociclib to letrozole slows the progression of advanced breast cancer and this combination and a number of other therapeutic strategies are being explored in the clinic [66].

5. Type I½ inhibitors

5.1. Type I½A inhibitors

Type I½ inhibitors bind reversibly within the ATP-binding pocket of an inactive DFG-Asp in conformation of their target protein kinases. Most of these inhibitors have the αC-helix out conformation with a distorted R-spine (Table 4). The type A subgroup occupies the front cleft and gate area and extends into the back cleft of the protein kinase whereas the type B subgroup occurs in the front cleft and gate area only as depicted in Fig. 4. Targets of the type A subgroup that are approved by the FDA include B-Raf, EGFR, Lyn, and VEGFR while targets of the type B subgroup include CDK2, EGFR, and c-Met.

Dasatinib is a type I½A inhibitor of Lyn that is approved for the treatment of Ph^+ (i) CML and (ii) ALL. Lyn is a member of the Src non-receptor protein-tyrosine kinase family [68]. It has both stimulatory and inhibitory effects depending upon the cellular context. Lyn is a signal transduction intermediary that is involved in a broad range of cellular functions such as apoptosis, cell division, cell migration, and differentiation. Like Src, Lyn has an N-terminal SH4 domain followed by an SH3 domain, an SH2 domain, and the Lyn kinase domain. Melanoma, colorectal, and prostate cancers represent other dasatinib disease targets [69]. Lyn expression has been linked to cancer progression and drug resistance [70] that may in part explain its effectiveness in the treatment of CML and ALL.

The amino group connecting the thiazole platform with the pyrimidine ring of dasatinib (Fig. 5D) makes one hydrogen bond with the carbonyl group of the Lyn hinge M322 of the mouse enzyme while the N3 nitrogen of the thiazole group makes another

hydrogen bond with the N—H group of M322. Furthermore, the amide nitrogen attached to the distal 2-chloro-6-methylphenyl group forms a hydrogen bond with the gatekeeper T319 and the distal group extends into the back cleft (Fig. 6L). On the whole dasatinib makes hydrophobic contacts with the β1-strand L253 before the G-rich loop, the β3C-spine A273 (CS8) and K275, RS3 M294, V303 of the back loop, I317 of the β5-strand before the hinge, ^{321}FMA^{323} of the hinge, L374 (CS6) within the β7-strand after the catalytic loop, and A384 that occurs just before the activation segment. The proximal pyrimidine ring of the drug extends out of the binding pocket through a cleft formed by L253 of the β1-strand and G325 of the hinge and the hydroxyethyl-piperazine group is largely solvent-exposed while making van der Waals contact with A323 of the hinge. Dasatinib inhibits several protein kinases, especially those of the Src family of which Lyn is one member (Table 3).

Lapatinib is a type I½A EGFR inhibitor with the DFG-D in and αC-helix out configuration. An α-helix near the beginning of the activation segment (αAS) helps to displace the αC-helix outward (Fig. 6M). Lapatinib is an FDA-approved medication for the first line treatment with letrozole for (i) post-menopausal women with hormone receptor positive metastatic breast cancer or (ii) for the second line treatment for women with breast cancer with the overexpression of ErbB2/HER2. Moreover, lapatinib is in clinical trials for the treatment of cervical, colorectal, gastroesophageal, head and neck squamous cell, prostate, thyroid, and uterine cancers as well as gliomas (www.clinicaltrials.gov) [31].

The N1 nitrogen of the quinazoline scaffold of lapatinib forms a hydrogen bond with the N—H group of M793 of the hinge while the β3-K745 makes polar contacts with DFG-D855 (Fig. 6M) [71]. The quinazoline scaffold is sandwiched from the top by the β3 C-spine A743 and from the bottom by the β7-strand C-spine L844, which occurs after the catalytic loop. The 3′-chloro-aniline group is positioned in a pocket formed by the side chains of CS7 V726 after the G-rich loop, the β3-K745, L788 of the β5-strand before the hinge, the gatekeeper T790, T854 immediately before the activation segment, and DFG-D855. The 3-fluorobenzyloxy group occupies a pocket formed by the side chains of the RS3 M766 of the R-spine, L777 at the beginning of the β4-strand, the gatekeeper T790, T854 before the activation segment, and DFG-F856 (RS2) and L858 within the activation segment. Furthermore, the DFG-D855 of VEGFR makes van der Waals contact with lapatinib.

Lapatinib also makes hydrophobic contacts with the β1-strand L781, Q791 and L792 of the hinge, and with the αD-helix CS3 L799 after the hinge. The aniline nitrogen and the ether oxygen are not involved in any direct hydrogen bonding interactions with the protein. The proximal methylsulfonylethylamino group is directed toward the solvent. The distal 3-chloro-4-[(3-fluorophenyl) methoxy]phenyl group of lapatinib extends into the back cleft of EGFR. Overall, lapatinib occupies BP-I-A/B in the gate area and "BP-II in" and the "BP-II-A in" sub-pockets of the back cleft (http://klifs.vu-compmedchem.nl/; PDB ID: 1XKK).

Vemurafenib is a type I½A inhibitor of B-Raf that is approved for the treatment of melanoma bearing the *BRAF*^{V600E} mutation, which occurs in about 50% of the patients with melanoma [72]. Vemurafenib occupies the adenine pocket with a DFG-D in conformation, thereby enabling the formation of hydrogen bond between the sulfonamide moiety and DFG-D595. A hydrogen bond is observed between the N7 N—H group of the pyrrolopyridine scaffold and the carbonyl group of the Q530 hinge residue and another hydrogen bond is observed between the N1 nitrogen of the scaffold and the N—H group of the C532 hinge residue (Fig. 6N), thereby mimicking that of the adenine core of ATP. The proximal 4-chlorophenyl group is exposed to the solvent. In addition, the distal 2,4-difluorophenyl propane-1-sulfonamide produces an outward shift of the regulatory αC-helix [73,74]. Overall, vemurafenib makes hydrophobic contacts with the β1-strand I463 before the G-rich loop, CS7 V471 after the G-rich loop, CS8 A481, RS3 L505, L514 of the αC-β4 loop, I527 of the β5-strand, the T529 gatekeeper, W531 of the hinge, CS6 F583, and RS2 DFG-F595. The drug also makes van der Waals contact with DFG-D594.

Vemurafenib was developed using a fragment-based drug discovery strategy that involved crystallographic studies of B-Raf bound to hundreds of compounds [74]. The name vemurafenib was derived from V600E mutated BRAF inhibition. The drug is in clinical trials for hormone refractory prostate cancer, thyroid cancer, other solid tumors, and Erdheim–Chester disease. The latter illness is characterized by the abnormal proliferation of immune cell histiocytes, which are derived from the bone marrow and migrate to blood as monocytes [75]. They circulate through the body and enter various organs, where they undergo differentiation into histiocytes. Long bone involvement is almost universal and bone pain is the most common symptom in Erdheim–Chester disease. About half these patients harbor point V600Q mutations of the *BRAF* gene, which provides the rationale for treating this illness with vemurafenib.

Thyroid cancer is the most common neoplasm of an endocrine organ. The most effective management of thyroid cancers is surgical removal of the thyroid gland (thyroidectomy) followed by radioactive iodine ablation and suppression by thyroid-stimulating hormone therapy. Lenvatinib is a type I½A inhibitor of VEGFR2 that is approved for the treatment of differentiated thyroid cancer, which is made up of papillary and follicular subtypes, that are locally recurrent or metastatic and not amenable to surgical excision. Targeting VEGFR is a common strategy for treating solid tumors [76], including thyroid cancer.

The lenvatinib-VEGFR2 complex contains one hydrogen bond linking the N1 nitrogen of the quinoline group of the drug (Fig. 5L) with the N—H group of C919 of the hinge, one hydrogen bond from each of the N—H groups of the urea connecting the cyclopropyl group and the 3-chlorophenoxy group with αC-E885, and a fourth hydrogen bond from the urea group carbonyl with the N—H group of DFG-D1046 (Fig. 6O) [77]. The distal cyclopropyl group interacts with the back cleft. On the whole, lenvatinib makes hydrophobic contacts with L840 within the G-rich loop, CS7 V844, the β3 CS8 A866 and K868, I888 and the RS3 L889 of the αC-helix, V899 of the back loop, V796 and F798 of the hinge, CS6 L1035, C1045 before the activation segment, RS2 DFG-F1047, and L1049 within the activation segment. Moreover, the DFG-D1046 of VEGFR2 makes van der Waals contact with the drug.

As lenvatinib binds to VEGFR2 in a DFG-D in conformation, a major conformational change is not required for drug dissociation and does not contribute to the extended drug-target residence time (Section 9). However, water-mediated interactions of its carbamoyl group with N923 of the hinge and of the cyclopropane ring with the back cleft may help to prolong the drug residence time. Okomoto et al. provide a classification of drug-protein kinase interactions and label lenvatinib as a type V inhibitor [77]. Their type V inhibitor with DFG-D in and the front cleft, gate area, and back cleft occupied corresponds to a type I½ inhibitor described by Zuccotto et al. [20] and a type I½A inhibitor in this paper. Lenvatinib is also an inhibitor of VEGFR1/3, FGFR1/2/3/4, Kit, PDGFRα, and RET and it is likely that its effectiveness is related to the inhibition of more than VEGFR2. However, it is also possible that its adverse effects may be due to the inhibition of one or more of these enzymes.

5.2. Type I½B inhibitors

Type I½B inhibitors bind reversibly within the ATP-binding pocket of an inactive DFG-Asp in conformation and occur in the front cleft and gate area but do not extend into the back cleft of protein kinases (Fig. 3, Table 4). Erlotinib is an FDA-approved medication for the second-line treatment of NSCLC and for the first-line

treatment of pancreatic cancer. It is a type I/I½B inhibitor of the EGFR receptor protein-tyrosine kinase. In its type I½B inhibition mode, the αC-helix is out and its E762 is far from the β3-K745 (Fig. 6P) [78]. Moreover, there is an αAS-helix that displaces the αC-helix outward. The N1 nitrogen of the quinazoline core makes a hydrogen bond with the N—H group of M793 of the hinge. The drug also makes hydrophobic contacts with the β1-strand L718 before the G-rich loop, the β2 CS7 V726 after the loop, the β3 CS8 A743 and K745, L788 of the β5-strand, and Q791, L792, and F795 of the hinge, the β7-strand CS6 L844, and T854 just before the activation segment. The 3-ethynyl group occupies BP-I-A and the phenyl group occupies BP-I-B in the gate area and the two methoxyethoxy groups extend into the solvent. Park et al. [78] note that their X-ray structure of erlotinib-EGFR (Fig. 6P) is very similar to that of lapatinib-EGFR with the lack of a salt bridge between the β3-K745 and αE-762 and the presence of an αAS helix that displaces the αC-helix outward (Fig. 6M).

As noted in Table 3, sunitinib is FDA-approved for the treatment of renal cell carcinomas, gastrointestinal stromal tumors, and progressive neuroendocrine tumors of pancreatic origin. The drug is a type I½B inhibitor of CDK2, a protein-serine/threonine kinase. CDK2 is activated by cyclins A, B, and E and participates in the G1/S transition [65]. The sunitinib-CDK2 complex contains a hydrogen bond connecting the N1 N—H group of the indolone scaffold of the drug (Fig. 5N) with the carbonyl group of E81 of the hinge, two polar contacts between the 2-oxo atom of the scaffold with the N—H group and carbonyl of L83 of the hinge, and one hydrogen bond between the carboxamide oxygen with the N—H group of D86 of the CDK2 hinge (Fig. 6Q) [79]. The drug makes hydrophobic contacts with the β1-strand I10, Y15 within the G-rich loop, CS7 V17 after the loop, CS8 A31, V64 of the αC-β4 loop, the gatekeeper F80, ^{82}FLHQ^{85} of the hinge, CS6 L134, and DFG-D145. The proximal triethylamine group projects toward the solvent and the distal fluoroindole group is directed toward the DFG-D145/β3-K33 motif. Sunitinib is also an inhibitor of several protein kinases and its clinical effectiveness may be related to its multiple targets (Table 3). However, such multikinase inhibition may contribute to the toxicity of the drug.

Crizotinib is FDA approved for the treatment of ALK$^+$ NSCLC; however, it was initially developed as a c-Met (hepatocyte growth factor receptor) antagonist [45,48]. c-Met signaling has been implicated in a wide variety of cancers including those of the breast, colon, liver, lung, stomach, prostate, and thyroid, and thus c-Met represents an attractive anticancer target [80]. Like many small molecule protein kinase inhibitors, crizotinib possesses both antiproliferative and antiangiogenic activities. See Ref [51] for a comprehensive description of the development of crizotinib as a combined c-Met and ALK inhibitor using a combination of X-ray crystal structural analyses and biological activity using lipophilic efficiency and ligand efficiency.

The amino group of the aminopyridine platform of crizotinib forms one hydrogen bond with the carbonyl group of the c-Met P1158 hinge and the N1 nitrogen of the pyridine ring forms another hydrogen bond with the N—H group of M1160 of the hinge (Fig. 6R) [51]. The α-methyl group and 2,6-dichloro moieties on the 3-benzyloxy group in crizotinib are critical for establishing the low nanomolar cell potency against c-Met. The R-methyl group not only stabilizes the benzyl group but also makes favorable hydrophobic interactions with CS7 V1092 after the G-rich loop, the gatekeeper L1157, and the β3 CS8 A1108 and K1110. The 5-pyrazol-4-yl group is bound through the narrow lipophilic tunnel surrounded by I1084 before the G-rich loop and Y1159 of the hinge. The distal 2,6-dichloro-3-fluorophenyl group of crizotinib is sandwiched between the β7-strand CS6 M1211 and Y1230 within the activation segment while occupying FP-I within the front cleft. The drug also makes hydrophobic contacts with L1140 of the back loop, N1209 within the catalytic loop, and A1221 just before the activation segment. Moreover, DFG-D1222 of c-Met makes van der Waals contact with crizotinib.

6. Type II inhibitors

6.1. Type IIA inhibitors

Type II inhibitors bind to the DFG-Asp out protein kinase conformation (Figs. 1F and 2 B), which corresponds to an inactive enzyme form. The RS2 phenylalanine of the R-spine is displaced from RS1 and RS3 as indicated in Table 4. Type IIB drugs occur within the front cleft and gate area while the type IIA drugs occur in the front cleft, gate area, and extend into the back cleft as depicted in Fig. 4. Owing to the uniqueness of inactive protein kinase conformations, it was hypothesized than type II drugs would be more selective than drugs that bind to the standard active conformation. However, there is considerable overlap of selectivity between type I and type II inhibitors so that perceived advantages of targeting inactive conformations have not been realized and binding mode analysis suggested that type II inhibitors do not show an intrinsic selectivity advantage over type I inhibitors [81].

Imatinib was the first FDA-approved small molecule protein kinase inhibitor and its success in the treatment of Ph$^+$ CML resulted in a paradigm shift indicating that small molecule protein kinase antagonists could target specific enzymes with little systemic toxicity [53]. Its importance in the subsequent development of small molecule protein kinases inhibitors cannot be overemphasized. Imatinib consists of a 2-phenylaminopyrimidine scaffold linked to a piperazinyl group and a pyridine linked via a peptide bond to a phenyl ring (Fig. 5O). Imatinib is a type IIA inhibitor of Abl that is approved by the FDA for the treatment of Ph$^+$ (i) CML and (ii) B-cell ALL, GIST, and several other illnesses (Table 3).

The N1 nitrogen of the pyridine group of imatinib forms a hydrogen bond with the N—H group of the Met318 hinge and the amino group of the tolylaminopyrimidine moiety forms a hydrogen bond with the –OH group of the Thr315 gatekeeper (Fig. 7A) [25]. Because the drug is bound to the DFG-Asp out conformation, this arrangement allows a hydrogen bond to form between the αC-E286 and the amide N—H group of imatinib and another is formed between the N—H group of DFG-D381 and the amide carbonyl oxygen of the drug (Fig. 7A) [25,53]. Moreover, the piperazinyl amine forms a bidentate linkage with His361 and Ile360 (Fig. 7A). Overall, the drug makes hydrophobic contacts with the β1-strand L248 before the G-rich loop, Y253 within the G-rich loop, and the β2 CS7 V256 after the G-rich loop, the β3 CS8 A269 and K271, V289 and RS3 M290 within the αC-helix, V299 within the αC-β4 loop, I313 within the β5-strand, F317 within the hinge, the β7-strand CS6 L370, A380 just before the activation segment, and RS2 DFG-F382. The tolyl group occupies the back cleft hydrophobic BP-II-out pocket and the distal piperazinylphenyl group binds to BP-IV that occurs in the DFG-Asp out configuration.

Imatinib is also a type IIA inhibitor of Kit and is approved for the treatment of GIST, most of which result from Kit activating mutations [82]. Kit is protein-tyrosine kinase that is the receptor for the stem cell factor (SCF), or Kit ligand [83]. This receptor participates in the regulation of apoptosis, gametogenesis, hematopoiesis, melanogenesis, cell proliferation, and stem cell maintenance. The receptor contains five extracellular immunoglobulin-like domains (IG1/2/3/4/5), a transmembrane segment, a juxtamembrane segment, and an intracellular protein kinase domain that contains an insert [84].

Imatinib makes the same four hydrogen bonds and the bidentate linkage with Kit that occur in Abl. The comparable Kit residues include the gatekeeper T670, C673 of the hinge, αC-E640, and DFG-

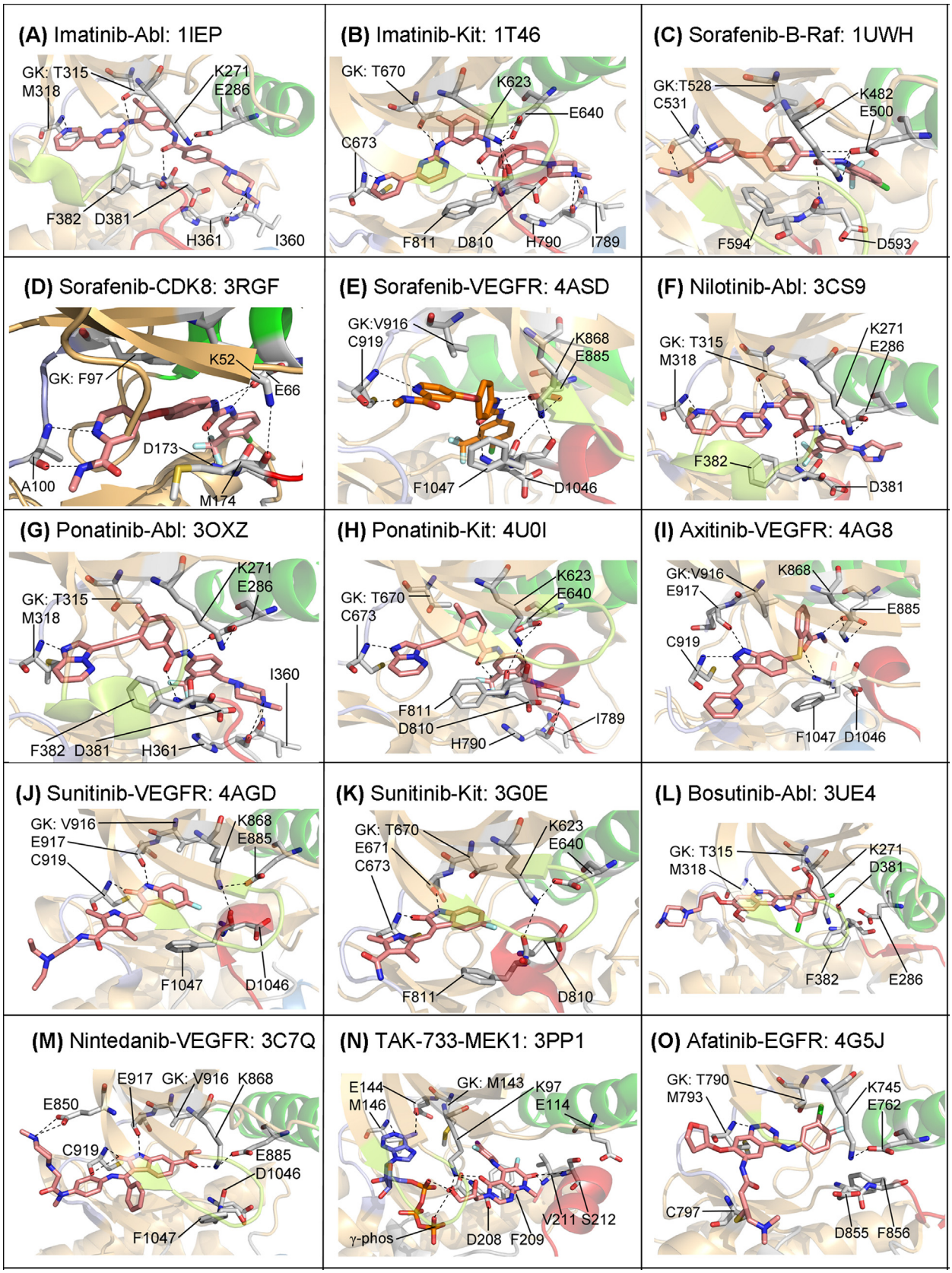

Fig. 7. Type IIA/B, III, and VI inhibitors. The protein kinase and corresponding PDB ID of each drug-enzyme complex are listed. The drug carbon atoms are orange, those of the enzyme are gray, and those of ATP (7N) are light blue. The dashed lines represent polar bonds. GK, gatekeeper.

D810 (Fig. 7B). The phenyl ring of imatinib occurs between the aliphatic portions of the side chains of DFG-D810, αC-E640 and L644, whereas the piperazine ring of the antagonist makes no specific interactions with the protein but rests in a shallow pocket bounded by V643 of the αC-helix, C788 and I789 before the catalytic loop, and the catalytic loop ^{790}HRD^{792}. Overall, the drug makes additional hydrophobic contacts with the β1-strand L595, CS7 V603, the β3 (i) CS8 A621, (ii) V622, (iii) K623, and (iv) M624, V643 and RS3 L644 within the αC-helix, V654 of the back loop, V668 of the β5-strand, Y672 of the hinge, R791 of the catalytic loop, CS6 L799, and RS2 DFG-F811 of the activation segment. Both the polar contacts and the overall hydrophobic interactions including those of the back cleft of imatinib with Abl (a non-receptor protein-tyrosine kinase) and Kit (a receptor protein-tyrosine kinase) are similar.

Sorafenib is an inhibitor of several protein kinases including the B-Raf and CDK8 protein-serine/threonine kinases and the VEGFR1/2/3 receptor protein-tyrosine kinases. The drug is an FDA-approved medication for the treatment of hepatocellular, renal cell, and differentiated thyroid carcinomas. B-Raf somatic missense mutations occur in 40–60% of malignant melanomas and in a wide range of human cancers at lower frequency including those of the colon, lung, and ovary [85]. B-Raf is an inducer of angiogenesis by promoting the expression of VEGF and it participates in pathways promoting cell migration and invasion [76]. The Raf family of kinases thus represents an attractive drug target in cancer therapy.

Sorafenib is a type IIA inhibitor of B-Raf; the latter is a member of the Ras/Raf/MEK/ERK signal transduction pathway that participates in cell proliferation. B-Raf thus participates in the transduction of mitogenic signals from the cell membrane to the nucleus. The N—H group of the picolinamide moiety (Fig. 5R) forms a hydrogen bond with the carbonyl group of the C531 B-Raf hinge while the N1 nitrogen of the pyridine group of the moiety forms a hydrogen bond with the N—H group of the same residue. Because the drug is bound to the DFG-Asp out conformation, this arrangement allows a hydrogen bond to form between the αC-E500 and each N—H group of the urea linker in sorafenib and another is formed between the N—H group of DFG-D593 and the carbonyl oxygen of the urea linker (Fig. 7C) [86]. The pyridyl ring of the antagonist occupies the front cleft AP pocket (Fig. 4) while interacting with three aromatic residues including W530 of the hinge region, the β7-strand CS6 F582, and RS2 DFG-F594. The trifluoromethyl phenyl ring of sorafenib inserts into a hydrophobic pocket formed by the αC- and αE-helices, the DFG signature sequence, and the catalytic loop. The aliphatic side chains of β3-K482, I512 and L513 of the αC-β4 loop, and the gatekeeper T528 contact the central phenyl ring of the antagonist. The drug also makes hydrophobic contacts with the β1-strand I462 before the G-rich loop, CS7 V470 after the G-rich loop, CS8 A480, V503 within the αC-helix, RS3 L504, L566 and I571 beneath the αC-helix and before the catalytic loop, RS1 HRD-H573 of the catalytic loop, and I591 before the activation segment. The 4-chloro-3-(trifluoromethyl) phenyl group makes hydrophobic contacts with BP-II-out and BP-III in that are located within the back cleft.

Sorafenib is also a type IIA inhibitor of the CDK8 protein-serine/threonine kinase. This enzyme is activated by cyclin C and participates in the regulated transcription of nearly all RNA polymerase II-dependent genes [65]. The activation segment of CDK8 begins with DMG in contrast to the usual DFG. The N—H group of the picolinamide moiety forms a hydrogen bond with the carbonyl group of the CDK8 hinge A100 while the N1 nitrogen of the pyridine group forms a hydrogen bond with the N—H group of the same residue. Sorafenib also forms two hydrogen bonds with αC-E66 and another one with DMG-D173 (Fig. 7D); these hydrogen bonds are analogous to those described above for B-Raf (Fig. 7C) [87]. The drug also makes hydrophobic contacts with the β2 CS7 V35, the β3 CS8 A50 and K52, the RS3 L70 and L73 of the αC-helix, V78 and I79 of the back loop, the F97 gatekeeper, Y99 of the hinge, L142 and V147 beneath the αC-helix and before the catalytic loop, RS1 HRD-H149 of the catalytic loop, I171 and A172 before the activation segment, and M174 and F176 of the activation segment. The 4-chloro-3-(trifluoromethyl) phenyl group makes hydrophobic contacts with BP-II-out and BP-III within the back cleft just as described above for B-Raf.

Sorafenib is also a type IIA inhibitor of the VEGFR1/2/3 protein-tyrosine kinases. This may explain in part its effectiveness in the treatment of RCC, tumors which are highly vascularized with a 90% incidence of Von Hippel-Lindau (VHL) tumor suppressor protein dysregulation [88]. With VHL inactivation, hypoxia inducible factor-α accumulates thereby leading to the overproduction of the VEGF angiogenic factor among others [76]. As a result, VEGFR inhibition accounts for the efficacy of these inhibitors in the treatment of RCC. Just as described above for its interaction with B-Raf, sorafenib forms two hydrogen bonds with C919 of the hinge, two with αC-E885, and one with DFG-D1046 (Fig. 7E). The drug also makes hydrophobic contacts with the β1-strand L840 before the G-rich loop, CS7 V848 after the G-rich loop, the β3 CS8 A866 and K868, the RS3 L889, I892 within the αC-helix, V899 within the αC-β4 loop, the V916 gatekeeper, F918 of the hinge, L1019 before the catalytic loop, RS1 HRD-H1026 of the catalytic loop, the β7-strand CS6 L1035, I1044 and C1045 just before the activation segment, and RS2 DFG-F1048. Sorafenib binds to the BP-I-B, II out, and III sub-pockets in the gate area and the back cleft of these three target proteins, the locations of which are illustrated in Fig. 4.

Nilotinib is a type IIA inhibitor of the Abl non-receptor protein-tyrosine kinase that is approved for the treatment of Ph$^+$ CML and was developed as a second-line medication for imatinib-resistant CML owing to point mutations in BCR–Abl, including E255V, M351T, and F486S. Nilotinib shares the same pyridine–pyrimidine–aminotolyl core as imatinib (Fig. 5O and 5P) [89]. The initial N1 nitrogen of pyridine of this second generation Abl inhibitor makes polar contacts with the M318 N—H group of the hinge while the N—H group of the aminotolyl group forms a hydrogen bond with the carbonyl oxygen of the —OH group of the T315 gatekeeper. The αC-E286 carboxylate forms a hydrogen bond with the amide N—H group connector in nilotinib and the DFG-D381 N—H group forms a hydrogen bond with the amide carbonyl oxygen (Fig. 7F). The latter two hydrogen bonds are possible because the protein kinase domain occurs in its DFG-Asp out conformation [20]. The drug also makes hydrophobic contacts with the β1-strand L248, Y253 within the G-rich loop, and CS7 V256 after the G-rich loop, the β3 CS8 A269 and K271, V289 and RS3 M290 of the αC-helix, I293, L298, and V299 of the back loop, I313 of the β5-strand, F317 of the hinge, F359 before the catalytic loop, RS1 HRD-H361 of the catalytic loop, CS6 L370, V379 and A380 just before the activation segment, and RS2 DFG-F382. The phenyl group makes hydrophobic contacts with BP-II-out while the imidazole methyl group occupies BP-III and the attached trifluoromethyl group occupies BP-V, all of which make it possible for nilotinib to bind deeply within the back pocket. Nilotinib is an effective antagonist against most Abl mutants, but not the common T315I gatekeeper mutation, the isoleucine of which blocks drug binding into the back cleft owing in part to the mutation of the small threonine residue to the bulky isoleucine residue.

Ponatinib is a third generation type IIA inhibitor of the non-receptor Abl protein-tyrosine kinase that is approved for Ph$^+$ (i) CML and (ii) ALL. The N1 nitrogen of the imidazo[1,2-*b*]pyridazine heterocycle of ponatinib (Fig. 5Q) forms a hydrogen bond with the N—H group of the Abl hinge M318 while the αC-E286 carboxylate forms a hydrogen bond with the N—H group of the amide linker and the DFG-D381 N—H group forms a hydrogen bond with the carbonyl oxygen of the linker. The N4 nitrogen of the methylpiper-

azine makes additional polar contacts with the carbonyl groups of I360 and HRD-H361 of the catalytic loop (Fig. 7G) [90]. In contrast to nilotinib, ponatinib fails to make a hydrogen bond with the Abl T315 gatekeeper and it is the only drug currently approved by the FDA that is effective against the Abl T315I gatekeeper mutant. Ponatinib makes hydrophobic contacts with the same residues as nilotinib noted above except for the β2 C-spine V256.

Ponatinib is a type IIA inhibitor of the Kit receptor protein-tyrosine kinase that is an approved medication for the treatment of Ph^+ (i) CML and (ii) ALL. Moore et al. reported that stem cell factor, the Kit ligand, stimulates proliferation in CML cells [91], leading to the possibility that Kit inhibition may be part of the ponatinib and nilotinib therapeutic response. Ponatinib makes polar contacts with C673 of the hinge, αC-E640, HRD-H790 of the catalytic loop, and DFG-D810 at the beginning of the activation segment, all of which parallel the interaction of the drug with Abl (Fig. 7H) [92]. It also makes hydrophobic contacts with the β1-strand L595 before the G-rich loop, CS7 V603, the β3 (i) CS8 A621, (ii) V622, and (iii) K623, RS3 L644 and L647 of the αC-helix, I653 and V654 of the αC-β4 loop, V668 of the β5-strand, the gatekeeper T670, Y672 of the hinge, R791 of the catalytic loop, CS6 L799, I808 and C809 before the activation segment, and RS2 DFG-F811of the activation segment. Ponatinib is a multikinase inhibitor that targets about one dozen protein kinases (Table 3). Imatinib, nilotinib, ponatinib, and sorafenib are Type IIA inhibitors that contain large aromatic components that interact with the various hydrophobic pockets in their target enzymes (Table 4).

Axitinib is a type IIA inhibitor of the VEGFR receptor protein-tyrosine kinase that is approved as a second line treatment for RCC. Axitinib is active against VEGFR1/2/3, PDGFRβ, and Kit. McTigue et al. studied the effects of the juxtamembrane (JM) domain on VEGFR2 enzymatic activity, autophosphorylation, and inhibition by axitinib, using kinetic, biophysical, and structural methodologies [88]. They prepared the VEGFR2 kinase domain with and without the upstream juxtamembrane segment and showed that the catalytic parameters for both constructs were similar, but the autophosphorylation rate of the enzyme with the juxtamembrane domain was faster than that lacking the domain. Moreover, they found that axitinib had a 40-fold enhanced biochemical potency toward the protein with the juxtamembrane domain compared with the enzyme lacking it. They reported that the properties of the protein with the juxtamembrane domain correlated closely with the cellular potency of axitinib. This study, which identified potential functions of the VEGFR2 juxtamembrane domain, emphasizes the importance of the nature of the protein construct used for mechanistic studies of receptor protein-tyrosine kinases and for the design of their inhibitors.

The N—H group of the indazole core of axitinib (Fig. 5S) forms a hydrogen bond with the E917 hinge carbonyl group and the N2 nitrogen of the core forms a hydrogen bond with the N—H group of the C919 hinge residue. Owing to the DFG-Asp out conformation, the αC-E885 carboxylate is able to form a hydrogen bond with the benzamide N—H group and the DFG-D1046 N—H group is able to form a hydrogen bond with the benzamide carbonyl oxygen (Fig. 7I). The drug also makes hydrophobic contacts with the β1-strand L840 proximal to the G-rich loop, the β2 CS7 V848 distal to the G-rich loop, the β3 CS8 A866 and K868, RS3 L889, V899 of the back loop, V914 of the β5-strand, the V916 gatekeeper, the hinge F918, and CS6 L1035 of the β7-strand, the C1045 preceding the activation segment, and RS2 DFG-F1047. The proximal pyridylvinyl chain extends toward the solvent and the distal benzamide group occupies BP-I-B in the gate area while the N-methyl group of benzamide extends into the back cleft. Axitinib is also an antagonist of PDGFRβ and its effectiveness against RCC may be due to the co-inhibition of this important enzyme. The X-ray crystal structure of PDGFRα/β has not yet been reported and such a determination represents a challenge for structural biologists.

6.2. Type IIB inhibitors

Type II inhibitors bind to the DFG-Asp out protein kinase conformation and type IIB drugs are restricted to the front cleft and gate area while the type IIA drugs occupy the front cleft, the gate area, and extend into the back cleft, all of which are depicted in Fig. 4. Sunitinib is an FDA-approved medication for the treatment of RCC, GIST, and progressive neuroendocrine tumors of pancreatic origin. The drug is a type IIB inhibitor of Kit and VEGFR2. The N—H group of the indolinone core of sunitinib makes one hydrogen bond with the E917 hinge carbonyl group and the ketone oxygen of the core makes another hydrogen bond with the N—H group of C919 of the VEGFR2 hinge (Fig. 7J) [93]. The drug also makes hydrophobic contacts with the β1-strand L840, CS8 A866, V899 of the αC-β4 loop, the gatekeeper V916, F918 of the hinge, CS6 L1035, C1054 just before the activation segment, and RS2 DFG-F1047. Renal cell carcinomas are highly vascular tumors and the effectiveness of sunitinib is ascribed in large part to the inhibition of VEGFR as noted above [76].

Sunitinib has been approved as a second-line therapy for patients with imatinib-resistant GIST (www.brimr.org/PKI/PKIs.htm). The effectiveness of sunitinib against GIST is due in large part to its ability to inhibit Kit. The drug binds only within the front pocket with the dihydrooxaindole ring occupying the adenine pocket in the front cleft. Sunitinib makes one hydrogen bond with the Kit E671 carbonyl group of the hinge (Fig. 7K) and another with the N—H group C673 of the hinge just as described above with VEGFR2 [93]. The drug also makes hydrophobic contacts with the β1-strand L595 before the G-rich loop, CS7 V603 after the G-rich loop, CS8 A621, V654 of the back loop, Y672 of the hinge, CS6 L799, C809 just before the activation segment, RS2 DFG-F811, and A814 of the activation segment. The proximal aliphatic diethylaminoethyl group is directed toward the solvent. Sunitinib is also an inhibitor of several protein kinases including PDGFRα/β, VEGFR1/2/3, Kit, Flt3, CSF-1R, and RET. Both the effectiveness of sunitinib and its adverse effects may be related to this large number of drug targets.

Bosutinib is a type I inhibitor of Src and type IIB inhibitor of Abl that is approved for the second line treatment of Ph^+ CML. The N1 quinoline nitrogen of this second generation Abl inhibitor forms one hydrogen bond with the N—H group of Abl M318 of the hinge (Fig. 7L) [62], which corresponds to its interaction with Src (Fig. 6A). The nitrile group extends into the gate area hydrophobic pocket BP-I-A near the Thr315 gatekeeper, which may host water molecules to form conserved water-mediated hydrogen bond interactions with small-molecule inhibitors that contribute to kinase selectivity [62]. The substituted aniline group of bosutinib occupies hydrophobic pocket BP-I-B within the gate area. In addition, bosutinib makes hydrophobic contacts with β1-strand L248 before the G-rich loop, the β3 (i) CS8 A269, (ii) A270, and (iii) K271, V299 of the αC-β4 loop, I313 of the β5 strand, the T314 gatekeeper, F317 and M318 of the hinge, the β7-strand CS6 L370, and DFG-F382 of the activation segment. Bosutinib interacts hydrophobically with the R-spine RS3 in Src but not in Abl; the drug interacts with DFG-F in Abl, but not in Src. Bosutinib is ineffective against the Abl T315I gatekeeper mutant. Owing to the propensity of BCR–Abl to adopt a certain conformation at the low pH values needed for crystallization, the DFG motif of the bosutinib-Abl complex exhibits a structure different from that of the dasatinib-Abl complex. A bosutinib-Src complex with the DFG motif adopting the same conformation as shown in the dasatinib-complex was described above [62].

Nintedanib is a small molecule protein kinase inhibitor that is approved for the treatment of idiopathic pulmonary fibrosis. This

illness is characterized by scarring of the lung and is accompanied by cough, dyspnea (difficulty of breathing), and progressive loss of lung function [94]. The median duration of survival after diagnosis is 2–3 years owing to the lack of effective therapies. The pathogenesis of this illness is unclear, but it is hypothesized to involve the action of the PDGFR, FGFR, and VEGFR protein-tyrosine kinases. Farkas et al. demonstrated that VEGF-A enhanced collagen expression induced by transforming growth factor-β in human lung fibroblasts [95]. As a VEGFR and multikinase inhibitor, the drug is in clinical trials for the treatment of HER2$^-$ inflammatory breast cancer, cervical, endometrial, and ovarian cancers, melanoma with wild-type *BRAF*, metastatic colorectal cancer, gastroesophageal and head and neck squamous cell cancers, and glioblastoma (www.clinicaltrials.gov).

Nintedanib is a type IIB inhibitor of VEGFR2, a receptor activated by VEGF-A [76]. The N—H group of the indolinone platform (Fig. 5T) forms one hydrogen bond with the E917 hinge carbonyl group and the ketone oxygen of the platform forms a hydrogen bond with the N—H group of the C919 hinge residue. The distal methyl ester carbonyl oxygen forms a hydrogen bond with the ϵ-amino group of β3-K868. The external solvent exposed N-methyl group of piperazine potentially forms two hydrogen bonds with the β2-E850 carboxylate group (Fig. 7M) [96]. Nintedanib makes hydrophobic contacts with the β1-strand L840, CS8 A866, V899 within the back loop, the gatekeeper V916, CS6 L1035, and C1045 occurring just before the activation segment. Nintedanib inhibits several protein kinases including FGFR1/2/3, Flt3, Lck, PDGFRα/β, and VEGFR1/2/3 [97]. Again, as a multikinase inhibitor, both the therapeutic and side effects of the drug may be related to these multiple targets.

7. Type III inhibitors

Type III inhibitors occupy a site next to the ATP-binding pocket (Table 2) so that both ATP and the allosteric inhibitor can bind simultaneously to the protein. These compounds are steady-state noncompetitive or uncompetitive inhibitors with respect to ATP because ATP cannot prevent their interaction with the enzyme. Type IV allosteric inhibitors bind to sites distant from the substrate binding sites. One example of a type IV inhibitor is GNF-2, an antagonist of BCR–Abl, which binds to the myristoyl binding site and stabilizes the inactive enzyme form [98]. Trametinib is a noncompetitive inhibitor of MEK1/2 with respect to ATP that is approved for the treatment of melanoma bearing mutant $BRAF^{V600E/K}$. The X-ray crystal structure of the complex of MEK1/2 with trametinib is not available so that TAK-733/MEK is used as an example. Note that TAK-733 is the only non-FDA approved medication whose X-ray structure is depicted in this paper.

TAK-733 binds to the MEK1-ATP complex in the gate area and the back cleft adjacent to the ATP-binding pocket. The pyridine ketone oxygen of the pyridopyrimidinedione scaffold (Fig. 5U) forms hydrogen bonds with the N—H groups of Val211 and Ser212 and the pyrimidine ketone oxygen interacts with the β3-strand K97. The hydroxyl groups of the distal 2,3-dihydroxypropyl chain each form a hydrogen bond with K97. The 3-hydroxyl group of the chain forms hydrogen bonds with both the α- and γ- phosphates of ATP (Fig. 7N) [99]. The drug also makes hydrophobic contacts with K97 and I99 of the β3-strand, L115 and L118 within the αC-helix, V127 within the αC-β4 loop, the β5-strand I141 before the hinge, the gatekeeper M143, RS2 DFG-F209, and V211, L215 and I216 within the activation segment. The drug binds in the gate area and back cleft, but it cannot bind to the adenine pocket owing to its occupation by ATP.

8. Type VI inhibitors

Type VI inhibitors are those drugs that bind covalently to their protein kinase target (Table 2). Afatinib and ibrutinib are currently FDA-approved drugs that form a covalent bond with their target. Afatinib inhibits EGFR (ErbB1), ErbB2, and ErbB4 and is approved for the treatment of NSCLC. Moreover, clinical trials with afatinib are underway for the treatment of HER2$^+$ breast and stomach cancers. Ibrutinib inhibits the Bruton non-receptor protein-tyrosine kinase and is approved for the treatment of mantle cell lymphoma, chronic lymphocytic leukemia, and Waldenström's macroglobulinemia (lymphoplasmacytic lymphoma). Ibrutinib clinical trials are underway for the treatment of breast cancer, CLL, NSCLC, and various lymphomas. Both of these compounds form Michael adducts with their target where a Michael reaction represents the addition of a nucleophile (the —SH of cysteine) to an α, β-unsaturated carbonyl compound [100]. The alkene portion of the drug forms a covalent bond with cysteine residues within the ATP-binding site. It is likely that noncovalent interactions position the small molecule in a productive orientation within the ATP-binding pocket that allows the covalent modification to proceed as the enzyme attacks the electrophilic portion of the drug.

The C3 carbon of the butanamide group of afatinib forms a covalent bond with C797 within the hinge of EGFR and the N1 nitrogen of the quinoline group forms one hydrogen bond with the N—H group of the M793 hinge residue (Fig. 7O) [101]. The drug also makes hydrophobic contacts with the β1-strand L718 before the G-rich loop, K728 after the G-rich loop, the β3 CS8 A743 and K745, the RS3 M766 of the R-spine, and L792 of the hinge, R841 within the distal catalytic loop (HRDLAARN), the β7-strand CS6 L844, and T854 just before the activation segment. The tetrahydro-3-furanyl group is exposed to the solvent and the 3-chloro-4-fluorophenyl-amino group (Fig. 5V) occurs in the gate area. Afatinib binds to the front cleft and gate area in the active conformation of EGFR. The Bruton protein kinase possesses a comparable C481 within its hinge, which is hypothesized to form a covalent link with ibrutinib.

9. Drug-target residence time

Drug-target interactions are generally characterized by equilibrium binding parameters such as the dissociation constant (K_d) or the concentration of drug that inhibits a process by 50% (IC_{50}) [102–104]. The dissociation constant is given by the following equation: $K_d = k_{off}/k_{on}$ where the thermodynamic K_d is related to the k_{off}/k_{on} kinetic rate constants, the numerator and denominator of which may consist of several components [102]. For weak binding interactions (K_d values in the millimolar-micromolar range) association and dissociation are usually rapid with half-lives in the microsecond time scale. This rapid binding and release are important for physiological processes such as enzyme catalysis. As the K_d decreases into the nanomolar range, the rates of association and dissociation may increase with values from seconds to minutes or hours. Copeland et al. introduced the concept of the drug-target residence time (τ) that can be approximated by the reciprocal of the dissociation rate constant according to the following equation: $\tau = 1/k_{off}$ [102]. The importance and mechanistic advantage is that drugs with a long target residence time are inhibitory at time points after the free drug has been eliminated from the cell.

Wood et al. studied the effects of three now FDA-approved EGFR antagonists (gefitinib, erlotinib, and lapatinib) on the duration of their inhibitory effects on human LICR-LON-HN5 cells expressing high levels of EGFR, which were initially derived from human squamous cell carcinomas of the oropharyngeal and laryngeal mucosa [71]. They found the following K_d values for EGFR: gefitinib, 0.4 nM; erlotinib, 0.7 nM; and lapatinib, 3.0 nM. The found that gefitinib

Table 5
Selected drug-target residence times.

Drug	Protein kinase target	Inhibitor type	Residence time	Reference
Sunitinib	VEGFR	IIB	<2.9 min	[77]
Gefitinib	EGFR	I	<10 min	[71]
Erlotiniib	EGFR	I/I½B	<10 min	[71]
Lenvatinib	VEGFR	I½A	17 min	[77]
Sorafenib	VEGFR	IIA	64 min	[77]
Lapatinib	EGFR	I½A	300 min	[71]
Sorafenib	B-Raf	IIA	568 min	[105]
Sorafenib	CDK8	IIA	576 min	[105]

and erlotinib had residence times of less than 10 min whereas lapatinib had a residence time of 300 min. After removing the drug from the HN5 cells after 4 h, these investigators found that lapatinib increased the duration of suppression of EGFR activity much longer than gefitinib or erlotinib in agreement with the residence time concept. However, the duration of action was much longer than expected from the residence time data (see [102] for possible mechanisms of the extended duration of the drug effects).

Wood et al. determined the X-ray crystal structure of these drugs with the EGFR protein kinase domain [71]. They found that the lapatinib binding pocket was much larger than that for the other two drugs and extends into what is now called the back pocket or cleft. They suggested that gefitinib and erlotinib have a shorter residence time owing to their dissociation from an active enzyme form without requiring any changes in protein conformation. They hypothesized that the dissociation of lapatinib from EGFR may require a receptor conformational change. Alternatively, the structure of lapatinib-EGFR may reflect a high binding affinity that results in a long residence time and slow-off rate without a need for a conformational change during inhibitor dissociation.

The residence times of a few other small molecule protein kinase inhibitors with their target are given in Table 5. Where the drug does not extend into the back cleft in the case of type I, I½B, and IIB inhibitors, the residence times are short. Where the drug extends into the back cleft in the case of type I½A and IIA inhibitors, the residence times are longer. These data include protein-tyrosine kinases and protein-serine/threonine kinases. Binding to the front cleft and gate area only is associated with a short residence time while binding to the back cleft is associated with a long residence time. Whether this correlation is found with other protein kinases and their antagonists remains to be established.

10. Epilogue

10.1. Rationale for the current classification of small molecule protein kinase inhibitors

The distinction between active and inactive conformations is a key concept in the protein kinase field. DFG-Asp in/out and αC-in/out represent the major conformational states [106]. Möbitz divided the DFG-Asp in conformations into three groups: (i) FG-down, (ii) DFG-active, and (iii) G-down. He also divided the DFG-Asp out conformations into three groups: (i) DFG-out type 2, (ii) DFG-flipped, (iii) A-under-P. He also noted that the αC-helix displays considerable conformational diversity. In the analysis provided in this paper, the nature of the regulatory spine was also taken into account in distinguishing active versus inactive conformations. Whereas a distinction of various DFG-Asp-in/out conformations may be difficult to discern by inspection, visualization of the structure of the R-spine removes most of these ambiguities. However, the classification of protein kinase structures and activity states in some instances is ambiguous.

van Linden et al. provided a comprehensive summary of drug and ligand binding to protein kinases based upon an analysis of more than 1200 structures derived from the protein data bank [24]. Their kinase–ligand interaction fingerprints and structure database (KLIFS), which contains an arrangement of 85 protein kinase ligand binding-site residues, facilitates the identification of group specific interaction features and classifies ligands according to the nature of their binding to target enzymes. They employ a generic residue numbering scheme throughout that allows a comparison among all protein kinases. The relationship between important residues documented in this paper and those of the KLIFS data base are listed in Table 6. Thus, KLIFS residue 11 corresponds to CS7, 15 to CS8, 28 to RS3, and 77 to CS6. Moreover, van Linden et al. have established an invaluable noncommercial searchable web site, which is continuously updated, that provides this information on human and mouse protein kinases (http://www.vu-compmedchem.nl/).

Table 6
Selected ligand-interacting residues in the protein kinase domain and KLIFS[a] generic numbered residues.

Location	KLIFS no.	KLIFS location
Before G-rich loop	3	I (β1-strand)
Within G-rich loop	4–9	G-rich loop (g.l.)
CS7 V	11	II (β2-strand)
CS8 A	15	III (β3-strand)
β3-K	17	III (β3-strand)
αC-E	24	αC-helix
RS3	28	αC-helix
αC-β4 loop	31-37	Back loop (b.l.)
Gatekeeper	45	Gatekeeper
Hinge	46–48	Hinge
αD-helix	53–59	αD-helix
αE-helix	60–64	αE-helix
Before catalytic loop	67	VI (β6-strand)
Catalytic loop[b]	68–75	Catalytic loop (c.l.)
CS6	77	VII (β7-strand)
Just before AS[c]	80	x
DFG	81–83	DFG
AS[c]	84–85	Activation loop (a.l.)

[a] From van Linden et al. [24].
[b] YRDLKPEN in the protein kinase AGC family [9].
[c] AS, activation segment.

The interaction of each drug with a protein kinase target is unique. Nevertheless, it is useful to classify these interactions in order to apply them to the drug discovery process. The classification outlined in Table 2 is adapted from that of previous authors [18,20–22] with more stringent criteria. For example, Dar and Shokat classify PP1 bound to Hck as a type I inhibitor [18]. However, the X-ray crystal structure shows that PP1 binds to the DFG-Asp in/αC-helix out conformation (PDB ID: 1QCF). The drug occupies the front cleft and gate area, but not the back pocket (klifs.vu-compmedchem.nl); we would classify PP1 as a type I½B inhibitor because the drug is bound to an inactive enzyme and does not extend into the back cleft. Similarly, Zuccotto et al. classify sunitinib as a type I inhibitor [20]. However, it binds to (i) the protein-serine/threonine CDK2 with the DFG-Asp in and αC-out conformation (PDB ID:3TIL) and it binds to (ii) the receptor protein-tyrosine kinases Kit (PDB ID: 3G0E) and VEGFR (PDB ID: 4AGD) with the DFG-Asp out and αC-helix out conformation. The drug occupies

the front cleft and the gate area, but not the back cleft. These correspond to type I½B and type IIB inhibitors in our classification, respectively. Essentially all classifications of type II inhibitors are in agreement; these drugs bind to an inactive DFG-Asp out configuration.

That a given inhibitor can bind to two different conformations of its targets adds to the complexity of inhibitor classification. Bosutinib is a type I inhibitor of Src and a type IIB inhibitor of Abl, both of which are protein-tyrosine kinases. Sunitinib is a type I½B inhibitor of CDK2 (a protein-serine/threonine kinase) and a type IIB inhibitor of Kit (a receptor protein-tyrosine kinase). Crizotinib is a type I inhibitor of ALK and a type I½ B inhibitor of c-Met, both of which are receptor protein-tyrosine kinases. Erlotinib is a type I and I½B inhibitor of EGFR, a receptor protein-tyrosine kinase. These results indicate that protein kinase antagonists are not necessarily conformationally selective. Moreover, these data suggest that drugs that occupy only the adenine pocket and gate area may be interchangeable as type I, I½B, and IIB inhibitors. By extrapolation, drugs that also occupy the back cleft may function as type I½A and IIA inhibitors, but not type I inhibitors.

We followed the suggestion of Gavrin and Saiah and subdivided the allosteric inhibitors into two categories (Table 2) [21]. The type III inhibitors bind to an allosteric site next to the adenine-binding pocket whereas the type IV inhibitors bind elsewhere. Lamba and Gosh classify type V inhibitors as those that bind to two different portions of the kinase lobe [22]. An ATP-analog peptide conjugate bound to the insulin receptor protein-tyrosine kinase domain as described by Parang et al., which extends from the ATP-binding pocket to the peptide/protein substrate binding site, is one example of a type V inhibitor [107]. All of these types of inhibitors are readily reversible. Covalent inhibitors generally bind irreversibly and whether they are classified as irreversible inhibitors, other, or type VI inhibitors is arbitrary.

10.2. New therapeutic indications for protein kinase inhibitors

We are only at the beginning of the era of targeting protein kinases for therapeutic purposes. Thus far only three dozen protein kinases represent bona fide drug targets (Tables 3) out of a family of more than 500 enzymes [1] and the number of targets is expected to increase. The FDA is approving small molecule protein kinase inhibitors at a rate of 2–4 per year and there is no sign that this will abate. Nearly all of the current therapeutic indications are for neoplastic diseases including leukemias, lymphomas, myelofibrosis, and various carcinomas. The approval of tofacitinib for the treatment of rheumatoid arthritis in 2012 and nintedanib for the treatment of idiopathic pulmonary fibrosis in 2014 represents an expanded therapeutic repertoire that we anticipate will multiply in the future. Cancers are characterized by genome instability and the development of resistance to both cytotoxic and targeted therapies [53]. Whether or not inflammatory disorders will display similar resistance to targeted therapies remains to be established.

Owing to the participation of protein kinases in a wide variety of physiological and pathological processes, one can foresee the use of targeted antagonists both as primary and secondary treatments for numerous illnesses. Besides rheumatoid arthritis and pulmonary fibrosis, we can expect the use of targeted protein kinase inhibitors as agents for the treatment, *inter alia,* of allograft rejection, asthma, hypertension, papilloma, Parkinson disease, psoriasis, and pulmonary hypertension [108,109]. The continued study of protein kinase structure and signal transduction pathways promises to yield new and useful information that will serve as a basis for fundamental and applied biomedical breakthroughs.

Conflict of interest

The author is unaware of any affiliations, memberships, or financial holdings that might be perceived as affecting the objectivity of this review.

Acknowledgment

The author thanks Laura M. Roskoski for providing editorial and bibliographic assistance.

References

[1] G. Manning, D.B. Whyte, R. Martinez, T. Hunter, S. Sudarsanam, The protein kinase complement of the human genome, Science 298 (2002) 1912–1934.
[2] A. Alonso, J. Sasin, N. Bottini, I. Friedberg, I. Friedberg, A. Osterman, et al., Protein tyrosine phosphatases in the human genome, Cell 117 (2004) 699–711.
[3] A. Bononi, C. Agnoletto, E. De Marchi, S. Marchi, S. Patergnani, M. Bonora, et al., Protein kinases and phosphatases in the control of cell fate, Enzyme Res. (2015), http://dx.doi.org/10.4061/2011/329098.
[4] P. Cohen, Protein kinases—the major drug targets of the twenty-first century? Nat. Rev. Drug Discov. 1 (2002) 309–315.
[5] R. Roskoski Jr., STI-571: an anticancer protein-tyrosine kinase inhibitor, Biochem. Biophys. Res. Commun. 309 (2003) 709–717.
[6] D.R. Knighton, J.H. Zheng, L.F. Ten Eyck, V.A. Ashford, N.H. Xuong, S.S. Taylor, et al., Crystal structure of the catalytic subunit of cyclic adenosine monophosphate-dependent protein kinase, Science 253 (1991) 407–414.
[7] D.R. Knighton, J.H. Zheng, L.F. Ten Eyck, N.H. Xuong, S.S. Taylor, J.M. Sowadski, Structure of a peptide inhibitor bound to the catalytic subunit of cyclic adenosine monophosphate-dependent protein kinase, Science 253 (1991) 414–420.
[8] S.S. Taylor, M.M. Keshwani, J.M. Steichen, A.P. Kornev, Evolution of the eukaryotic protein kinases as dynamic molecular switches, Philos. Trans. R. Soc. Lond. B Biol. Sci. 367 (2012) 2517–2528.
[9] S.K. Hanks, A.M. Quinn, T. Hunter, The protein kinase family: conserved features and deduced phylogeny of the catalytic domains, Science 241 (1988) 42–52.
[10] H.S. Meharena, P. Chang, M.M. Keshwani, K. Oruganty, A.K. Nene, N. Kannan, et al., Deciphering the structural basis of eukaryotic protein kinase regulation, PLoS Biol. 11 (2013) e1001680.
[11] B. Nolen, S. Taylor, G. Ghosh, Regulation of protein kinases; controlling activity through activation segment conformation, Mol. Cell 15 (2004) 661–675.
[12] N. Gotoh, A. Tojo, M. Hino, Y. Yazaki, M. Shibuya, A highly conserved tyrosine residue at codon 845 within the kinase domain is not required for the transforming activity of human epidermal growth factor receptor, Biochem. Biophys. Res. Commun. 186 (1992) 768–774.
[13] D.A. Tice, J.S. Biscardi, A.L. Nickles, S.J. Parsons, Mechanism of biological synergy between cellular Src and epidermal growth factor receptor, Proc. Natl. Acad. Sci. U. S. A. 96 (1999) 1415–1420.
[14] M. Huse, J. Kuriyan, The conformational plasticity of protein kinases, Cell 109 (2002) 275–282.
[15] A.P. Kornev, N.M. Haste, S.S. Taylor, L.F. Ten Eyck, Surface comparison of active and inactive protein kinases identifies a conserved activation mechanism, Proc. Natl. Acad. Sci. U. S. A. 103 (2006) 17783–17788.
[16] A.P. Kornev, S.S. Taylor, L.F. Ten Eyck, A helix scaffold for the assembly of active protein kinases, Proc. Natl. Acad. Sci. U. S. A. 105 (2008) 14377–14382.
[17] J. Zhang, P.L. Yang, N.S. Gray, Targeting cancer with small molecule kinase inhibitors, Nat. Rev. Cancer 9 (2009) 28–39.
[18] A.C. Dar, K.M. Shokat, The evolution of protein kinase inhibitors from antagonists to agonists of cellular signaling, Annu. Rev. Biochem. 80 (2011) 769–795.
[19] J. Monod, J.P. Changeux, F. Jacob, Allosteric proteins and cellular control systems, J. Mol. Biol. 6 (1963) 306–329.
[20] F. Zuccotto, E. Ardini, E. Casale, M. Angiolini, Through the gatekeeper door: exploiting the active kinase conformation, J. Med. Chem. 53 (2010) 2681–2694.
[21] L.K. Gavrin, E. Saiah, Approaches to discover non-ATP site inhibitors, Med. Chem. Commun. 4 (2013) 41.
[22] V. Lamba, I. Ghosh, New directions in targeting protein kinases: focusing upon true allosteric and bivalent inhibitors, Curr. Pharm. Des. 18 (2012) 2936–2945.
[23] J.J. Liao, Molecular recognition of protein kinase binding pockets for design of potent and selective kinase inhibitors, J. Med. Chem. 50 (2007) 409–424.
[24] O.P. van Linden, A.J. Kooistra, R. Leurs, I.J. de Esch, C. de Graaf, KLIFS: a knowledge-based structural database to navigate kinase-ligand interaction space, J. Med. Chem. 57 (2014) 249–277.
[25] B. Nagar, W.G. Bornmann, P. Pellicena, T. Schindler, D.R. Veach, W.T. Miller, et al., Crystal structures of the kinase domain of c-Abl in complex with the small molecule inhibitors PD173955 and imatinib (STI-571), Cancer Res. 62 (2002) 4236–4243.

[26] D. Fabbro, S.W. Cowan-Jacob, H. Moebitz, Ten things you should know about protein kinases: IUPHAR review 14, Br. J. Pharmacol. 172 (2015) 2675–2700.
[27] P.Y. Yip, Phosphatidylinositol 3-kinase-AKT-mammalian target of rapamycin (PI3K-Akt-mTOR) signaling pathway in non-small cell lung cancer, Transl. Lung Cancer Res. 4 (2015) 165–176.
[28] S. Romano, A. D'Angelillo, M.F. Romano, Pleiotropic roles in cancer biology for multifaceted proteins FKBPs, Biochim. Biophys. Acta 1850 (2015) 2061–2068.
[29] H. Yang, D.G. Rudge, J.D. Koos, B. Vaidialingam, H.J. Yang, N.P. Pavletich, mTOR kinase structure, mechanism and regulation, Nature 497 (2013) 217–223.
[30] R. Roskoski Jr., The ErbB/HER receptor protein–tyrosine kinases and cancer, Biochem. Biophys. Res. Commun. 319 (2004) 1–11.
[31] R. Roskoski Jr., The ErbB/HER family of protein-tyrosine kinases and cancer, Pharmacol. Res. 79 (2014) 34–74.
[32] R. Roskoski Jr., ErbB/HER protein-tyrosine kinases: structures and small molecule inhibitors, Pharmacol. Res. 87 (2014) 42–59.
[33] C.H. Yun, K.E. Mengwasser, A.V. Toms, M.S. Woo, H. Greulich, K.K. Wong, et al., The T790M mutation in EGFR kinase causes drug resistance by increasing the affinity for ATP, Proc. Natl. Acad. Sci. U. S. A. 105 (2008) 2070–2075.
[34] C.H. Yun, T.J. Boggon, Y. Li, M.S. Woo, H. Greulich, M. Meyerson, et al., Structures of lung cancer-derived EGFR mutants and inhibitor complexes: mechanism of activation and insights into differential inhibitor sensitivity, Cancer Cell 11 (2007) 217–227.
[35] F. Ciardiello, R. Caputo, R. Bianco, V. Damiano, G. Pomatico, S. De Placido, et al., Antitumor effect and potentiation of cytotoxic drugs activity in human cancer cells by ZD-1839 (Iressa), an epidermal growth factor receptor-selective tyrosine kinase inhibitor, Clin. Cancer Res. 6 (2000) 2053–2063.
[36] P.M. Ellis, N. Coakley, R. Feld, S. Kuruvilla, Y.C. Ung, Use of the epidermal growth factor receptor inhibitors gefitinib, erlotinib, afatinib, dacomitinib, and icotinib in the treatment of non-small-cell lung cancer: a systematic review, Curr. Oncol. 22 (2015) e183–e215.
[37] J. Stamos, M.X. Sliwkowski, C. Eigenbrot, Structure of the epidermal growth factor receptor kinase domain alone and in complex with a 4-anilinoquinazoline inhibitor, J. Biol. Chem. 277 (2002) 46265–46272.
[38] A. Cid-Arregui, V. Juarez, Perspectives in the treatment of pancreatic adenocarcinoma, World J. Gastroenterol. 21 (2015) 9297–9316.
[39] J.D. Rowley, Letter: a new consistent chromosomal abnormality in chronic myelogenous leukaemia identified by quinacrine fluorescence and Giemsa staining, Nature 243 (1973) 290–293.
[40] J. Groffen, J.R. Stephenson, N. Heisterkamp, A. de Kein, C.R. Bartram, G. Grosveld, Philadelphia chromosomal breakpoints are clustered within a limited region, bcr, on chromosome 22, Cell 36 (1984) 93–99.
[41] E. Jabbour, H. Kantarjian, J. Cortes, Use of second- and third-generation tyrosine kinase inhibitors in the treatment of chronic myeloid leukemia: an evolving treatment paradigm, Clin. Lymphoma Myeloma Leuk. 15 (2015) 323–334.
[42] J.S. Tokarski, J.A. Newitt, C.Y. Chang, J.D. Cheng, M. Wittekind, S.E. Kiefer, et al., The structure of Dasatinib (BMS-354825) bound to activated ABL kinase domain elucidates its inhibitory activity against imatinib-resistant ABL mutants, Cancer Res. 66 (2006) 5790–5797.
[43] T. O'Hare, D.K. Walters, E.P. Stoffregen, T. Jia, P.W. Manley, J. Mestan, et al., *In vitro* activity of Bcr–Abl inhibitors AMN107 and BMS-354825 against clinically relevant imatinib-resistant Abl kinase domain mutants, Cancer Res. 65 (2005) 4500–4505.
[44] N.P. Shah, C. Tran, F.Y. Lee, P. Chen, D. Norris, C.L. Sawyers, Overriding imatinib resistance with a novel ABL kinase inhibitor, Science 305 (2004) 399–401.
[45] M.S. Mathisen, H.M. Kantarjian, J. Cortes, E.J. Jabbour, Practical issues surrounding the explosion of tyrosine kinase inhibitors for the management of chronic myeloid leukemia, Blood Rev. 28 (2014) 179–187.
[46] M.A. Lemmon, J. Schlessinger, Cell signaling by receptor tyrosine kinases, Cell 141 (2010) 1117–1134.
[47] R. Roskoski Jr., Anaplastic lymphoma kinase (ALK): structure, oncogenic activation, and pharmacological inhibition, Pharmacol. Res. 68 (2013) 68–94.
[48] R. Roskoski Jr., The preclinical profile of crizotinib for the treatment of non-small-cell lung cancer and other neoplastic disorders, Expert. Opin. Drug Discov. 8 (2013) 1165–1179.
[49] M. Soda, Y.L. Choi, M. Enomoto, S. Takada, Y. Yamashita, S. Ishikawa, et al., Identification of the transforming EML4–ALK fusion gene in non–small–cell lung cancer, Nature 448 (2007) 561–566.
[50] K. Rikova, A. Guo, Q. Zeng, A. Possemato, J. Yu, H. Haack, et al., Global survey of phosphotyrosine signaling identifies oncogenic kinases in lung cancer, Cell 131 (2007) 1190–1203.
[51] J.J. Cui, M. Tran-Dubé, H. Shen, M. Nambu, P.P. Kung, M. Pairish, et al., Structure based drug design of crizotinib (PF-02341066), a potent and selective dual inhibitor of mesenchymal-epithelial transition factor (c-MET) kinase and anaplastic lymphoma kinase (ALK), J. Med. Chem. 54 (2011) 6342–6363.
[52] M.A. Davare, N.A. Vellore, J.P. Wagner, C.A. Eide, J.R. Goodman, A. Drilon, et al., Structural insight into selectivity and resistance profiles of ROS1 tyrosine kinase inhibitors, Proc. Natl. Acad. Sci. U. S. A. 112 (2015) E5381–E5390.
[53] R. Roskoski Jr., A historical overview of protein kinases and their targeted small molecule inhibitors, Pharmacol. Res. 100 (2015) 1–23.
[54] B.C. Liao, C.C. Lin, J.Y. Shih, J.C. Yang, Treating patients with ALK-positive non-small cell lung cancer: latest evidence and management strategy, Ther. Adv. Med. Oncol. 7 (2015) 274–290.
[55] L. Friboulet, N. Li, R. Katayama, C.C. Lee, J.F. Gainor, A.S. Crystal, et al., The ALK inhibitor ceritinib overcomes crizotinib resistance in non-small cell lung cancer, Cancer Discov. 4 (2014) 662–673.
[56] A. Quintás-Cardama, K. Vaddi, P. Liu, T. Manshouri, J. Li, P.A. Scherle, et al., Preclinical characterization of the selective JAK1/2 inhibitor INCB018424: therapeutic implications for the treatment of myeloproliferative neoplasms, Blood 115 (2010) 3109–3117.
[57] B.L. Stein, S.T. Oh, D. Berenzon, G.S. Hobbs, M. Kremyanskaya, R.K. Rampal, C.N. Abboud, et al., Polycythemia vera: an appraisal of the biology and management 10 years after the discovery of JAK2 V617F, J. Clin. Oncol. (2015), pii: JCO.2015.61.6474.
[58] Y. Duan, L. Chen, Y. Chen, X.G. Fan, c-Src binds to the cancer drug ruxolitinib with an active conformation, PLoS One 9 (2014) e106225.
[59] P.P. Knowles, J. Murray-Rust, S. Kjaer, R.P. Scott, S. Hanrahan, M. Santoro, et al., Structure and chemical inhibition of the RET tyrosine kinase domain, J. Biol. Chem. 281 (2006) 33577–33587.
[60] P. Fallahi, F. Di Bari, S.M. Ferrari, R. Spisni, G. Materazzi, P. Miccoli, et al., Selective use of vandetanib in the treatment of thyroid cancer, Drug Des. Dev. Ther. 9 (2015) 3459–3470.
[61] A. Morabito, M.C. Piccirillo, F. Falasconi, G. De Feo, A. Del Giudice, J. Bryce, et al., Vandetanib (ZD6474), a dual inhibitor of vascular endothelial growth factor receptor (VEGFR) and epidermal growth factor receptor (EGFR) tyrosine kinases: current status and future directions, Oncologist 14 (2009) 378–390.
[62] N.M. Levinson, S.G. Boxer, A conserved water-mediated hydrogen bond network defines bosutinib's kinase selectivity, Nat. Chem. Biol. 10 (2014) 127–132.
[63] J.E. Chrencik, A. Patny, I.K. Leung, B. Korniski, T.L. Emmons, T. Hall, et al., Structural and thermodynamic characterization of the TYK2 and JAK3 kinase domains in complex with CP-690550 and CMP-6, J. Mol. Biol. 400 (2010) 413–433.
[64] N.K. Williams, R.S. Bamert, O. Patel, C. Wang, P.M. Walden, A.F. Wilks, et al., Dissecting specificity in the Janus kinases: the structures of JAK-specific inhibitors complexed to the JAK1 and JAK2 protein tyrosine kinase domains, J. Mol. Biol. 387 (2009) 219–232.
[65] M. Malumbres, Cyclin-dependent kinases, Genome Biol. 15 (2014) 122.
[66] K.A. Cadoo, A. Gucalp, T.A. Traina, Palbociclib: an evidence-based review of its potential in the treatment of breast cancer, Breast Cancer (Dove Med. Press) 6 (2014) 123–133.
[67] H. Lu, U. Schulze-Gahmen, Toward understanding the structural basis of cyclin-dependent kinase 6 specific inhibition, J. Med. Chem. 49 (2006) 3826–3831.
[68] R. Roskoski Jr., Src protein-tyrosine kinase structure, mechanism, and small molecule inhibitors, Pharmacol. Res. 94 (2015) 9–25.
[69] J.C. Montero, S. Seoane, A. Ocaña, A. Pandiella, Inhibition of Src family kinases and receptor tyrosine kinases by dasatinib: possible combinations in solid tumors, Clin. Cancer Res. 17 (2011) 5546–5552.
[70] M.A. Eldeeb, R.P. Fahlman, The anti-apoptotic form of tyrosine kinase Lyn that is generated by proteolysis is degraded by the N-end rule pathway, Oncotarget 5 (2014) 2714–2722.
[71] E.R. Wood, A.T. Truesdale, O.B. McDonald, D. Yuan, A. Hassell, S.H. Dickerson, et al., A unique structure for epidermal growth factor receptor bound to GW572016 (Lapatinib): relationships among protein conformation, inhibitor off-rate, and receptor activity in tumor cells, Cancer Res. 64 (2004) 6652–6659.
[72] R. Roskoski Jr., ERK1/2 MAP kinases: structure, function, and regulation, Pharmacol. Res. 66 (2012) 105–143.
[73] G. Bollag, P. Hirth, J. Tsai, J. Zhang, P.N. Ibrahim, H. Cho, et al., Clinical efficacy of a RAF inhibitor needs broad target blockade in *BRAF* -mutant melanoma, Nature 467 (2010) 596–599.
[74] G. Bollag, J. Tsai, J. Zhang, C. Zhang, P. Ibrahim, K. Nolop, P. Hirth, Vemurafenib: the first drug approved for *BRAF* -mutant cancer, Nat. Rev. Drug Discov. 11 (2012) 873–886.
[75] R.D. Mazor, M. Manevich-Mazor, Y. Shoenfeld, Erdheim–Chester disease: a comprehensive review of the literature, Orphanet J. Rare Dis. 8 (2013) 137.
[76] R. Roskoski Jr., Vascular endothelial growth factor (VEGF) signaling in tumor progression, Crit. Rev. Oncol. Hematol. 62 (2007) 179–213.
[77] K. Okamoto, M. Ikemori-Kawada, A. Jestel, K. von König, Y. Funahashi, T. Matsushima, et al., Distinct binding mode of multikinase inhibitor lenvatinib revealed by biochemical characterization, ACS Med. Chem. Lett. 6 (2014) 89–94.
[78] J.H. Park, Y. Liu, M.A. Lemmon, R. Radhakrishnan, Erlotinib binds both inactive and active conformations of the EGFR tyrosine kinase domain, Biochem. J. 448 (2012) 417–423.
[79] M.P. Martin, R. Alam, S. Betzi, D.J. Ingles, J.Y. Zhu, E. Schönbrunn, A novel approach to the discovery of small-molecule ligands of CDK2, Chembiochem 13 (2012) 2128–2136.
[80] C. Birchmeier, W. Birchmeier, E. Gherardi, G.F. Vande Woude, Met, metastasis, motility and more, Nat. Rev. Mol. Cell Biol. 4 (2003) 915–925.

[81] Z. Zhao, H. Wu, L. Wang, Y. Liu, S. Knapp, Q. Liu, N.S. Gray, Exploration of type II binding mode: a privileged approach for kinase inhibitor focused drug discovery? ACS Chem. Biol. 9 (2014) 1230–1241.
[82] R. Roskoski Jr., Structure and regulation of Kit protein-tyrosine kinase–the stem cell factor receptor, Biochem. Biophys. Res. Commun. 338 (2005) 1307–1315.
[83] R. Roskoski Jr., Signaling by Kit protein-tyrosine kinase–the stem cell factor receptor, Biochem. Biophys. Res. Commun. 337 (2005) 1–13.
[84] C.D. Mol, D.R. Dougan, T.R. Schneider, R.J. Skene, M.L. Kraus, D.N. Scheibe, et al., Structural basis for the autoinhibition and STI-571 inhibition of c-Kit tyrosine kinase, J. Biol. Chem. 279 (2004) 31655–31663.
[85] H. Davies, G.R. Bignell, C. Cox, P. Stephens, S. Edkins, S. Clegg, et al., Mutations of the *BRAF* gene in human cancer, Nature 417 (2002) 949–954.
[86] P.T. Wan, M.J. Garnett, S.M. Roe, S. Lee, D. Niculescu-Duvaz, V.M. Good, et al., Mechanism of activation of the RAF-ERK signaling pathway by oncogenic mutations of B-RAF, Cell 116 (2004) 855–867.
[87] E.V. Schneider, J. Böttcher, M. Blaesse, L. Neumann, R. Huber, K. Maskos, The structure of CDK8/CycC implicates specificity in the CDK/cyclin family and reveals interaction with a deep pocket binder, J. Mol. Biol. 412 (2011) 251–266.
[88] M. McTigue, B.W. Murray, J.H. Chen, Y.L. Deng, J. Solowiej, R.S. Kania, Molecular conformations, interactions, and properties associated with drug efficiency and clinical performance among VEGFR TK inhibitors, Proc. Natl. Acad. Sci. U. S. A. 109 (2012) 18281–18289.
[89] E. Weisberg, P.W. Manley, W. Breitenstein, J. Brüggen, S.W. Cowan-Jacob, A. Ray, et al., Characterization of AMN107, a selective inhibitor of native and mutant Bcr–Abl, Cancer Cell 7 (2005) 129–141.
[90] T. Zhou, L. Commodore, W.S. Huang, Y. Wang, M. Thomas, J. Keats, et al., Structural mechanism of the Pan–BCR–ABL inhibitor ponatinib (AP24534): lessons for overcoming kinase inhibitor resistance, Chem. Biol. Drug Des. 77 (2011) 1–11.
[91] S. Moore, D.N. Haylock, J.P. Lévesque, L.A. McDiarmid, L.M. Samels, L.B. To, et al., Stem cell factor as a single agent induces selective proliferation of the Philadelphia chromosome positive fraction of chronic myeloid leukemia $CD34^+$ cells, Blood 92 (1998) 2461–2470.
[92] A.P. Garner, J.M. Gozgit, R. Anjum, S. Vodala, A. Schrock, T. Zhou, et al., Ponatinib inhibits polyclonal drug-resistant KIT oncoproteins and shows therapeutic potential in heavily pretreated gastrointestinal stromal tumor (GIST) patients, Clin. Cancer Res. 20 (2014) 5745–5755.
[93] K.S. Gajiwala, J.C. Wu, J. Christensen, G.D. Deshmukh, W. Diehl, J.P. DiNitto, et al., KIT kinase mutants show unique mechanisms of drug resistance to imatinib and sunitinib in gastrointestinal stromal tumor patients, Proc. Natl. Acad. Sci. U. S. A. 106 (2009) 1542–1547.
[94] M. Inomata, Y. Nishioka, Azuma A. Nintedanib, evidence for its therapeutic potential in idiopathic pulmonary fibrosis, Core Evid. 10 (2015) 89–98.
[95] L. Farkas, D. Farkas, K. Ask, A. Möller, J. Gauldie, P. Margetts, et al., VEGF ameliorates pulmonary hypertension through inhibition of endothelial apoptosis in experimental lung fibrosis in rats, J. Clin. Invest. 119 (2009) 1298–1311.
[96] F. Hilberg, G.J. Roth, M. Krssak, S. Kautschitsch, W. Sommergruber, U. Tontsch-Grunt, et al., BIBF 1120: triple angiokinase inhibitor with sustained receptor blockade and good antitumor efficacy, Cancer Res. 68 (2008) 4774–4782.
[97] G.J. Roth, R. Binder, F. Colbatzky, C. Dallinger, R. Schlenker-Herceg, F. Hilberg, et al., Nintedanib: from discovery to the clinic, J. Med. Chem. 58 (2015) 1053–1063.
[98] F.J. Adrián, Q. Ding, T. Sim, A. Velentza, C. Sloan, Y. Liu, et al., Allosteric inhibitors of Bcr–Abl-dependent cell proliferation, Nat. Chem. Biol. 2 (2006) 95–102.
[99] Q. Dong, D.R. Dougan, X. Gong, P. Halkowycz, B. Jin, T. Kanouni, et al., Discovery of TAK-733, a potent and selective MEK allosteric site inhibitor for the treatment of cancer, Bioorg. Med. Chem. Lett. 21 (2011) 1315–1319.
[100] P.A. Schwartz, B.W. Murray, Protein kinase biochemistry and drug discovery, Bioorg. Chem. 39 (2011) 192–210.
[101] F. Solca, G. Dahl, A. Zoephel, G. Bader, M. Sanderson, C. Klein, et al., Target binding properties and cellular activity of afatinib (BIBW 2992), an irreversible ErbB family blocker, J. Pharmacol. Exp. Ther. 343 (2012) 342–350.
[102] R.A. Copeland, D.L. Pompliano, T.D. Meek, Drug-target residence time and its implications for lead optimization, Nat. Rev. Drug. Discov. 5 (2006) 730–739.
[103] P.J. Tummino, R.A. Copeland, Residence time of receptor-ligand complexes and its effect on biological function, Biochemistry 47 (2008) 5481–5492, Erratum in: Biochemistry 2008; 47: 8465.
[104] R.A. Copeland, Conformational adaptation in drug-target interactions and residence time, Future Med. Chem. 3 (2011) 1491–1501.
[105] L. Neumann, K. von König, D. Ullmann, HTS reporter displacement assay for fragment screening and fragment evolution toward leads with optimized binding kinetics, binding selectivity, and thermodynamic signature, Methods Enzymol. 493 (2011) 299–320.
[106] H. Möbitz, The ABC of protein kinase conformations, Biochim. Biophys. Acta 2015 (1854) 1555–1566.
[107] K. Parang, J.H. Till, A.J. Ablooglu, R.A. Kohanski, S.R. Hubbard, P.A. Cole, Mechanism-based design of a protein kinase inhibitor, Nat. Struct. Biol. 8 (2001) 37–41.
[108] P. Cohen, D.R. Alessi, Kinase drug discovery––what's next in the field? ACS Chem. Biol. 8 (2013) 96–104.
[109] A. Levitzki, Tyrosine kinase inhibitors: views of selectivity, sensitivity, and clinical performance, Annu. Rev. Pharmacol. Toxicol. 53 (2013) 161–185.